

20005  
11/11/52  
NACA TN 2816

# NATIONAL ADVISORY COMMITTEE FOR AERONAUTICS

TECHNICAL NOTE 2816

WATER-PRESSURE DISTRIBUTIONS DURING LANDINGS OF  
A PRISMATIC MODEL HAVING AN ANGLE OF  
DEAD RISE OF  $22\frac{1}{2}^{\circ}$  AND BEAM-LOADING  
COEFFICIENTS OF 0.48 AND 0.97

By Robert F. Smiley

Langley Aeronautical Laboratory  
Langley Field, Va.

## DISTRIBUTION STATEMENT A

Approved for Public Release  
Distribution Unlimited



Reproduced From  
Best Available Copy

Washington  
November 1952

20000508 233

M00-08-2264

## NATIONAL ADVISORY COMMITTEE FOR AERONAUTICS

## TECHNICAL NOTE 2816

## WATER-PRESSURE DISTRIBUTIONS DURING LANDINGS OF

A PRISMATIC MODEL HAVING AN ANGLE OF

DEAD RISE OF  $22\frac{1}{2}^{\circ}$  AND BEAM-LOADING

COEFFICIENTS OF 0.48 AND 0.97

By Robert F. Smiley

## SUMMARY

Smooth-water landing tests of a prismatic model having an angle of dead rise of  $22\frac{1}{2}^{\circ}$  were made as part of a landing investigation being conducted at the Langley impact basin to determine the distribution of water pressure on seaplanes. Landings were made for beam-loading coefficients of 0.48 and 0.97 at fixed trims between  $0.2^{\circ}$  and  $30.3^{\circ}$  for a range of initial flight-path angles from  $4.6^{\circ}$  to  $25.9^{\circ}$  and also for  $90^{\circ}$ .

Initial impact conditions, over-all loads and motions, and maximum pressures are presented in tables and figures for all the landings, together with instantaneous-pressure-distribution and wave-rise data.

The experimental wave rise, peak pressures, and pressure distributions are found to be in fair agreement with the predictions of the available theory; however, better agreement is obtained by modification of the theory.

## INTRODUCTION

In order to obtain information regarding the magnitude and distribution of the water-pressure distribution during seaplane landings, an experimental program is being conducted at the Langley impact basin on various prismatic models. The results of investigations on heavily loaded prismatic models having angles of dead rise of  $0^{\circ}$  and  $30^{\circ}$  have been reported in references 1 and 2, respectively. The present investigation was made on a lightly loaded prismatic model having beam-loading coefficients of 0.48 and 0.97, an angle of dead rise of  $22\frac{1}{2}^{\circ}$ , and a beam

of 3.39 feet. Fixed-trim landings were made in smooth water for a large range of trims, velocities, and flight-path angles. During each landing, time histories of the pressures, velocities, draft, and over-all loads were recorded.

The purpose of this paper is to present the experimental pressure-distribution, velocity, draft, wave-rise, and over-all-loads data obtained from this investigation and to use these data to evaluate and extend the existing knowledge of the wave rise and pressure distribution on V-bottom seaplanes. Pressure distributions are compared to show the effects of flight-path angle and beam loading, and experimental wave-rise and pressure data are compared with the available theoretical and empirical predictions that are summarized in references 3 and 4. In addition these theories are modified in order to obtain better agreement with the experimental data.

#### SYMBOLS

A	hydrodynamic aspect ratio $\left( \frac{(\text{Wetted length at keel})^2}{\text{Wetted area projected normal to keel}} \right)$
b	beam of model, feet
c	wetted semiwidth at any station along keel, feet
f̄	equivalent planing velocity, feet per second $(\dot{f} = \dot{x} + \dot{y} \cot \tau = \frac{\dot{z}}{\sin \tau})$
F <sub>N</sub>	hydrodynamic force normal to keel (normal to surface for a flat plate), pounds
g	acceleration due to gravity, 32.2 feet per second per second
J	empirical function of angle of dead rise
K	transverse-wave-rise ratio $\left( \frac{\tan \delta_2}{\tan \delta_1} \right)$
n <sub>i_w</sub>	impact acceleration normal to undisturbed water surface, $g$ units $\left( -\frac{\ddot{z} \cos \tau}{g} \right)$

p	instantaneous pressure, pounds per square inch
t	time after water contact, seconds
v	instantaneous resultant velocity of model, feet per second
w	weight of model and dropping weight, pounds
$\dot{x}$	instantaneous velocity of model parallel to undisturbed water surface, feet per second
y	instantaneous draft of model normal to undisturbed water surface, feet
$\dot{y}$	instantaneous velocity of model normal to undisturbed water surface, feet per second
$\ddot{z}$	instantaneous velocity of model normal to keel, feet per second $(\dot{x} \sin \tau + \dot{y} \cos \tau)$
$\ddot{z}$	instantaneous acceleration of model normal to keel, feet per second per second $\left( -\frac{n_i w g}{\cos \tau} \right)$
$\beta$	angle of dead rise, degrees
$\gamma$	instantaneous flight-path angle relative to undisturbed water surface, degrees $\left( \tan^{-1} \frac{\dot{y}}{\dot{x}} \right)$
$\delta_1, \delta_2$	angles used to designate wave rise, degrees
$\xi$	distance forward of step, measured parallel to keel, feet
$\eta$	transverse distance from keel, feet
$\theta$	effective angle of dead rise, degrees
$\lambda_d$	length of keel below undisturbed water surface, beams $\left( \frac{y}{b \sin \tau} \right)$
$\lambda_p$	wetted length based on peak-pressure location (longitudinal distance from step to position of peak pressure at keel), beams

$\rho$  mass density of water, 1.938 slugs per cubic foot

$\tau$  trim, degrees

Subscripts:

$o$  at water contact

max at maximum value

p at peak pressure

Dimensionless variables:

$C_N$  normal-load coefficient for a rectangular flat plate based  
on  $A$ ;  $\left( \frac{F_N}{\frac{1}{2} \rho f^2 b^2 A} \right)$

$C_{N_p}$  normal-load coefficient for a rectangular flat plate based  
on  $\lambda_p$ ;  $\left( \frac{F_N}{\frac{1}{2} \rho f^2 b^2 \lambda_p} \right)$

$C_\Delta$  beam-loading coefficient  $\left( \frac{W}{\rho g b^3} \right)$

$\frac{p}{\frac{1}{2} \rho f z^2}$  pressure coefficient based on  $z$

#### APPARATUS

The investigation was conducted in the Langley impact basin with the test equipment described in reference 5. The test model was a forebody of a seaplane float, substantially prismatic in shape as shown in figure 1.

The prismatic section had an angle of dead rise of  $22\frac{1}{2}^\circ$ .

The instrumentation used to measure horizontal velocity and vertical velocity at water contact is described in reference 5. Accelerations in the vertical direction were measured with two oil-damped strain-gage-type accelerometers having approximately 0.65 of the critical damping. One

accelerometer had a range from -12g to 12g and a natural frequency of 120 cycles per second while the other had a range from -10g to 10g and a natural frequency of 100 cycles per second. Both instruments were recorded by 0.65 critically damped galvanometers having natural frequencies of 100 cycles per second. Vertical velocity after water contact was obtained by integration of the vertical acceleration. Draft was obtained by double integration of the vertical acceleration. The instants of water contact and exit of the model were determined by means of an electrical circuit completed by the water. Pressures were measured with 43 gages distributed over the hull bottom as shown in figure 2 and table I. Forty-two of these gages had flat diaphragms of  $\frac{1}{2}$ -inch diameter which were mounted flush with the hull bottom; the other was a bellows-type gage with a  $\frac{1}{4}$ -inch-diameter pickup surface. Natural frequencies of the pressure gages were several thousand cycles per second and the response of the oscillograph recording system was accurate to frequencies up to slightly more than 1000 cycles per second.

In order to evaluate properly the experimental accelerometer data (and the derived velocity and draft data), the dynamic response characteristics of the accelerometers and the corresponding recording galvanometers had to be taken into account. Analysis of this dynamic response for the experimental conditions of these tests showed that the response characteristics of the accelerometer-galvanometer circuit were of such a nature that the magnitude of the recorded accelerations should be reasonably accurate but that the recorded traces were displaced in time by approximately 0.005 second. All the data presented in this paper have been corrected for this time lag.

#### PRECISION

The instrumentation used in these tests gives measurements that are estimated to be usually accurate within the following limits:

Horizontal velocity, feet per second . . . . .	$\pm 0.5$
Vertical velocity at water contact, feet per second . . . . .	$\pm 0.2$
Vertical velocity after water contact, feet per second . . . . .	$\pm 0.5$
Vertical acceleration, percent . . . . .	$\pm 5$
Pressure, pounds per square inch . . . . .	$\pm 2 \pm 0.1p$
Time, seconds . . . . .	$\pm 0.005$
Draft, feet . . . . .	$\pm 0.03$

### TEST PROCEDURE

A series of 30 landings were made in smooth water with the model at  $0^\circ$  yaw and at various fixed trims. Sixteen landings were made with the model loaded to a weight of 1177 pounds, which corresponded to a beam-loading coefficient of 0.48. For these landing runs the model was tested at trims of  $0.2^\circ$ ,  $3.2^\circ$ ,  $6.3^\circ$ ,  $9.3^\circ$ ,  $12.4^\circ$ ,  $20.5^\circ$ , and  $30.3^\circ$  for a range of initial flight-path angles from  $4.6^\circ$  to  $25.9^\circ$  and also for  $90^\circ$ . Fourteen landings were made with the model loaded to a weight of 2369 pounds, which corresponded to a beam-loading coefficient of 0.97. For these landing runs the model was tested at trims of  $0.2^\circ$ ,  $6.3^\circ$ ,  $12.4^\circ$ ,  $15.4^\circ$ ,  $20.5^\circ$ , and  $30.3^\circ$  for a range of initial flight-path angles from approximately  $5^\circ$  to  $15^\circ$  and also for  $90^\circ$ .

During each landing a compressed-air engine (described in reference 5) exerted a vertical lift force on the model equal to the test weight so that the model simulated a seaplane with wing lift equal to the weight of the seaplane. Otherwise the model was free to move in the vertical direction. The model was attached to a towing carriage weighing approximately 5400 pounds in such a manner that it could not move horizontally with respect to the carriage. Because of this large additional carriage inertia, the model did not slow down very much (horizontally) during any landing.

### EXPERIMENTAL RESULTS

The initial vertical, horizontal, and resultant velocities, flight-path angles, trims, and model weights for all landings are presented in table II together with the experimental over-all loads and motions. Time histories of the vertical velocity are presented in table III. The corresponding instantaneous horizontal velocities are substantially the same as the initial values given in table II since the change in horizontal velocity during any impact was small. The values of the maximum pressures recorded on each pressure gage are presented for all runs in table IV and the corresponding times of maximum pressure are presented in table V. The peak-pressure data for two runs are plotted against  $\frac{1}{2}p_z^2$  in figure 3. The average value of the peak-pressure coefficient

cient  $\frac{p_p}{\frac{1}{2}p_z^2}$  (see faired lines in fig. 3) as obtained from similar plots

for other runs are plotted against trim in figure 4 for all runs. In table VI are given instantaneous-pressure-distribution data from most

of these landings together with the corresponding measurements of time, draft, vertical velocity, and vertical acceleration. Illustrative pressure distributions are plotted in figure 5 for various trims.

Transverse-wave-rise measurements, as defined by the following equation, are shown in figure 6 for trims between  $3.2^\circ$  and  $15.4^\circ$ :

$$K = \frac{\tan \delta_2}{\tan \delta_1} \quad (1)$$

The angles  $\delta_1$  and  $\delta_2$  are shown in figure 7(a),  $\delta_1$  being given by the relation

$$\tan \delta_1 = \tan \tau \cot \beta$$

The angle  $\delta_2$  was obtained from observations of the experimental pressure distributions (from table VI) or of the position of the peak pressure on the float (from table V). For trims greater than approximately  $15^\circ$ , an examination of unpublished underwater photographs obtained at Langley tank no. 1 for a planing prism having an angle of dead rise of  $20^\circ$  indicates that the peak-pressure line is curved; therefore, equation (1) is not valid. Consequently, no wave-rise ratios are shown for the trims larger than  $15.4^\circ$ .

## ANALYSIS OF RESULTS

### Wave Rise

During the impact or planing of a V-bottom prismatic model, the water rises above the level water surface. The forward component of this rise ( $\lambda_p - \lambda_d$  in fig. 7(a)) is usually small. The transverse wave rise, however, is usually large. This transverse wave rise is defined by the location of the peak-pressure line on the hull bottom, which is close to the boundary of the wetted area (see fig. 7). For small trims (up to approx.  $15^\circ$  according to the previously mentioned unpublished planing data for a model having an angle of dead rise of  $20^\circ$ ), this peak-pressure line is substantially straight and can be conveniently described by the ratio  $K$ . Pierson and Leshover have proposed the following equation for  $K$  in reference 4:

$$K \approx \frac{\pi}{2} \left( 1 - \frac{3 \tan^2 \beta \cos \beta}{1.7\pi^2} - \frac{\tan \beta \sin^2 \beta}{3.3\pi} \right) \quad (2)$$

This theoretical variation is compared with the experimental data of this paper in figure 6. Fair agreement is seen to exist.

### Peak Pressures

Several equations have been proposed for the peak pressure on V-bottom wedges having a finite angle of trim. Two of the most promising of these equations are considered and a third more accurate equation is proposed. The following equation was derived by Pierson and Leshnover in reference 4:

$$\frac{P_p}{\frac{1}{2}\rho z^2} = \frac{(K - \sin^2 \beta)^2}{\sin^2 \beta + K^2 \tan^2 \tau} + \cos^2 \beta \quad (3)$$

where  $K$  is given by equation (2). Equation (3) is based upon a theoretical analysis concerned with the peak-pressure line. If such a line exists reasonable results might be expected from this equation. However, for very large trims no such line exists (see fig. 7) and this analysis does not hold. For example at  $90^\circ$  trim equation (3) predicts

$$\frac{P_p}{\frac{1}{2}\rho z^2} = \cos^2 \beta$$

whereas a more accurate relation is

$$\frac{P_p}{\frac{1}{2}\rho z^2} = 1 \quad (4)$$

(see reference 2). In order to determine the value of equation (3) for an angle of dead rise of  $22\frac{1}{2}^\circ$ , computed and experimental peak pressures are compared in figure 4. It is seen that this equation is conservative for trims below approximately  $10^\circ$  and is fairly reasonable for trims between  $10^\circ$  and  $30^\circ$ .

A second equation which has been proposed for the peak pressure is the following semiempirical equation proposed in reference 2:

$$\frac{P_p}{\frac{1}{2}\rho z^2} = \frac{1}{\sin^2\tau + \frac{4}{\pi^2} \tan^2\beta \cos^2\tau} \quad (5)$$

This equation is an empirical relation which was chosen to satisfy the theoretical relation given by equation (4) for  $90^\circ$  trim, to satisfy the following theoretical relation given by Wagner

$$\frac{P_p}{\frac{1}{2}\rho z^2} = \frac{\pi^2}{4} \cot^2\beta \quad (\tau = 0^\circ; \beta \rightarrow 0^\circ) \quad (6)$$

and to satisfy the experimental variation of the peak pressure with trim for a model having a  $30^\circ$  angle of dead rise (reference 2). Comparisons of the predictions of equation (5) with the experimental peak-pressure data from this paper for an angle of dead rise of  $22\frac{1}{2}^\circ$  (shown in fig. 4) indicate that, for this angle of dead rise, equation (5) is conservative throughout the trim range.

Since neither equation (3) nor equation (5) is always in close agreement with the experimental data, a third equation is proposed here as

$$\frac{P_p}{\frac{1}{2}\rho z^2} = \frac{1}{\sin^2\tau + J^2 \cos^2\tau} \quad (7)$$

where  $J$  is considered to be a function of angle of dead rise alone. Equation (7) was obtained by replacing the quantity  $\frac{2}{\pi} \tan \beta$  in equation (5) by a more general quantity  $J$ . In order to satisfy equation (6) and to agree with the experimental data of reference 2,  $J$  must have the values  $\frac{2}{\pi} \tan \beta$  for  $\beta \rightarrow 0^\circ$  and  $\tau = 0^\circ$  and for  $\beta = 30^\circ$  for all trims so that for these cases equations (5) and (7) are identical. For other angles of dead rise,  $J$  can be determined either empirically or from

theoretical solutions for the two-dimensional case for which equation (7) reduces to the relation

$$\frac{p}{\frac{1}{2} \rho \dot{z}^2} = \frac{1}{J^2} \quad (\tau = 0^\circ)$$

For an angle of dead rise of  $22\frac{1}{2}^\circ$ , an examination of the experimental data in this paper indicated that the value of  $J$  that best fits the data is 0.293. Computed peak pressures based on this value of  $J$  are compared with the experimental pressures in figure 4. Reasonable agreement is seen to exist for all trims.

#### Pressure Distribution

Effects of beam loading and flight-path angle. - Experimental pressure-distribution data for various trims are shown in figure 5 in the form of the dimensionless pressure coefficient  $\frac{p}{\frac{1}{2} \rho \dot{z}^2}$ . The effect of beam loading

on these pressure coefficients is shown in figures 5(a) and 5(b) where experimental data for the same trim, wetted area, and flight-path angle and different beam-loading coefficients are superimposed. It appears that there is little difference in the experimental pressure coefficients for the two beam loadings tested. The effect of flight-path angle on the pressure coefficients is shown in figures 5(c) and 5(d) where experimental data for the same trim, wetted area, and beam-loading coefficient and different flight-path angles are superimposed. No apparent effect of flight-path angle on the pressure coefficients is noted. This conclusion is in agreement with the results of reference 2 for a model with a  $30^\circ$  angle of dead rise.

Non-chine-immersed region. - For the transverse pressure distribution on non-chine-immersed sections of a two-dimensional V-bottom wedge (see fig. 7) during a zero-trim constant-velocity impact, Wagner (see reference 6 or 7) has obtained an equation which can be expressed as

$$\frac{p}{\frac{1}{2} \rho \dot{z}^2} = \frac{\pi \cot \beta}{\sqrt{1 - \left(\frac{n}{c}\right)^2}} - \frac{1}{\left(\frac{c}{n}\right)^2 - 1}$$

In order to extend this equation to apply to the case of a finite trim, Pierson and Leshner (reference 4) have proposed that this equation be replaced by the equation

$$\frac{p_p}{\frac{1}{2} \rho z^2} = \frac{\pi \cot \theta}{\sqrt{1 - \left(\frac{\eta}{c}\right)^2}} - \frac{1}{\left(\frac{c}{\eta}\right)^2 - 1} \quad (8)$$

The maximum value of equation (8) is given by the relation

$$\left. \begin{aligned} \frac{p_p}{\frac{1}{2} \rho z^2} &= \left( \frac{\pi}{2} \cot \theta \right)^2 + 1 && (\pi \cot \theta \geq 2) \\ \frac{p_p}{\frac{1}{2} \rho z^2} &= \pi \cot \theta && (\pi \cot \theta \leq 2) \end{aligned} \right\} \quad (9)$$

This relation defines  $\theta$  in terms of the peak pressure. Different values of  $\theta$  can be obtained by substituting equations (3), (5), and (7) into equation (9):

The value obtained from equation (3), which will be designated as  $\theta_1$ , is

$$\pi \cot \theta_1 = 2 \sqrt{\frac{K^2 - 2K \sin^2 \beta - K^2 \sin^2 \beta \tan^2 \tau}{\sin^2 \beta + K^2 \tan^2 \tau}} \quad (\pi \cot \theta_1 \geq 2)$$

$$\pi \cot \theta_1 = \frac{(K - \sin^2 \beta)^2}{\sin^2 \beta + K^2 \tan^2 \tau} + \cos^2 \beta \quad (\pi \cot \theta_1 \leq 2)$$

The value obtained from equation (5), which will be designated as  $\theta_2$ , is

$$\pi \cot \theta_2 = 2 \sqrt{\frac{1 - \frac{4}{\pi^2} \tan^2 \beta}{\tan^2 \tau + \frac{4}{\pi^2} \tan^2 \beta}} \quad (\pi \cot \theta_2 \geq 2)$$

$$\pi \cot \theta_2 = \frac{1}{\sin^2 \tau + \frac{4}{\pi^2} \tan^2 \beta \cos^2 \tau} \quad (\pi \cot \theta_2 \leq 2)$$

The value obtained from equation (7), which will be designated as  $\theta_3$ , is

$$\pi \cot \theta_3 = 2 \sqrt{\frac{1 - J^2}{\tan^2 \tau + J^2}} \quad (\pi \cot \theta_3 \geq 2)$$

$$\pi \cot \theta_3 = \frac{1}{\sin^2 \tau + J^2 \cos^2 \tau} \quad (\pi \cot \theta_3 \leq 2)$$

For the usual case of impacts not made at constant velocity, as a first approximation the following term, which takes into account the acceleration normal to the keel and which is usually negative (see reference 3), should be added to equation (8)

$$\frac{2\ddot{z}_c \phi(A)}{\dot{z}^2} \sqrt{1 - \left(\frac{\eta}{c}\right)^2} \quad (10)$$

where

$$\phi(A) = \sqrt{\frac{1}{1 + \frac{1}{A^2}}} \left(1 - \frac{0.425}{A + \frac{1}{A}}\right) \quad (0 < A < \infty)$$

$$\phi(A) = 1 - \frac{1}{2A} \quad (1.5 < A < \infty)$$

and

$$A = \frac{(\text{Wetted length at keel})^2}{\text{Wetted area projected normal to keel}}$$

so that equation (8) becomes

$$\frac{p}{\frac{1}{2}\rho z^2} = \frac{\pi \cot \theta}{\sqrt{1 - \left(\frac{\eta}{c}\right)^2}} - \frac{1}{\left(\frac{c}{\eta}\right)^2 - 1} + \frac{2z c \varphi(A)}{z^2} \sqrt{1 - \left(\frac{\eta}{c}\right)^2} \quad (11)$$

Theoretical pressure distributions computed according to equation (11) for the non-chine-immersed region of the model are shown in figure 5 below the corresponding experimental pressure distributions. Most of these pressure distributions were computed by using  $\theta_3$  with  $J = 0.293$ . It is seen that on the non-chine-immersed region of the float bottom these pressure distributions computed by using  $\theta_3$  are in fair agreement with the experimental data for all trims. The pressure distribution computed by using  $\theta_1$  is shown in figure 5(a) for a trim of  $0.2^\circ$ . As would be expected from the peak-pressure analysis (see fig. 4), this equation leads to pressures larger than the experimental pressure for this trim. However, for larger trims (not shown) there is little difference between the pressures predicted by using  $\theta_1$  and  $\theta_3$ . For all trims, predictions of the pressure distribution based on  $\theta_2$  (not shown) are conservative approximately to the same extent as the peak-pressure predictions of equation (5) are conservative (see fig. 4). It is noted that the theoretical effect of beam loading on the pressure distribution (which effect is given by expression (10)) appears to be greater than the experimental effect.

Chine-immersed region. - A semiempirical procedure for predicting the pressure distribution on the chine-immersed region of a prismatic V-bottom wedge (fig. 7(b)) has been given in reference 3. It should be noted that this procedure requires a knowledge of the normal-load coefficient  $C_{N_p}$  of a rectangular flat plate as a function of trim and wetted length. For trims below  $16^\circ$  this variation can be found from figure 9 of reference 3. For larger trims the following equation, which can be obtained from the analysis of reference 8, can be used

$$C_N = \frac{\varphi(A) \sin \tau \cos \tau \left( \frac{\pi^3}{16} + 0.88A \tan \tau \right)}{A}$$

Usually  $A \approx \lambda_p$  so that  $C_N$  is approximately equal to the quantity  $C_{N_p}$  used in the analysis of reference 3. From the evidence presented in reference 3 for a model having a  $30^\circ$  angle of dead rise, it appears that this procedure gives reasonable results for cases where the chine-immersed wetted area of the model is a large fraction of the total wetted area.

Pressure distributions on the chine-immersed region of the float computed according to this semiempirical procedure are shown in figure 5 below the corresponding experimental pressure distributions. It is seen that where the chine-immersed wetted area is not too small a fraction of the total wetted area (figs. 5(d) and 5(e)) fair agreement exists.

#### CONCLUDING REMARKS

From an analysis of the experimental data obtained during a smooth-water landing investigation of a substantially prismatic float having an angle of dead rise of  $22\frac{1}{2}^{\circ}$  and beam-loading coefficients of 0.48 and 0.97, it is seen that the experimental wave rise is in fair agreement with the theoretical prediction of Pierson and Leshnover.

Comparisons of computed and experimental peak pressures indicate that the peak-pressure equation advanced by Pierson and Leshnover appears to be conservative for trims below  $10^{\circ}$  and to be in reasonable agreement with the experimental data for trims between  $10^{\circ}$  and  $30^{\circ}$ . The peak-pressure equation advanced in NACA TN 2111 appears to be conservative for all trims. A third peak-pressure equation advanced herein appears to be in reasonable agreement with the experimental data for all trims.

An examination of the experimental pressure distributions indicates that there is no effect of flight-path angle on the pressure coefficients based on the velocity normal to the keel and that there is little difference in the experimental pressure coefficients for the two beam loadings tested. In non-chine-immersed regions of the float, computed pressure distributions corresponding to the three peak-pressure equations mentioned compare with the experimental pressure distributions in much the same manner as for the respective peak pressures. In chine-immersed regions of the float where the chine-immersed wetted area is not too small a fraction of the total wetted area, computed pressure distributions are in fair agreement with the experimental results.

Langley Aeronautical Laboratory  
National Advisory Committee for Aeronautics  
Langley Field, Va., January 10, 1952

## REFERENCES

1. Smiley, Robert F.: An Experimental Study of Water-Pressure Distributions During Landings and Planing of a Heavily Loaded Rectangular Flat-Plate Model. NACA TN 2453, 1951.
2. Smiley, Robert F.: A Study of Water Pressure Distributions During Landings With Special Reference to a Prismatic Model Having a Heavy Beam Loading and a 30° Angle of Dead Rise. NACA TN 2111, 1950.
3. Smiley, Robert F.: A Semiempirical Procedure for Computing the Water-Pressure Distribution on Flat and V-Bottom Prismatic Surfaces During Impact or Planing. NACA TN 2583, 1951.
4. Pierson, John D., and Leshnover, Samuel: A Study of the Flow, Pressures, and Loads Pertaining to Prismatic Vee-Planing Surfaces. S.M.F. Fund Paper No. FF-2, Inst. Aero. Sci. (Rep. No. 382, Project No. NR 062-012, Office of Naval Res., Exp. Towing Tank, Stevens Inst. Tech.), May 1950.
5. Batterson, Sidney A.: The NACA Impact Basin and Water Landing Tests of a Float Model at Various Velocities and Weights. NACA Rep. 795, 1944. (Supersedes NACA ACR L4H15.)
6. Pierson, John D.: On the Pressure Distribution for a Wedge Penetrating a Fluid Surface. Preprint No. 167, S.M.F. Fund Paper, Inst. Aero. Sci. (Rep. No. 336, Project No. NR 062-012, Office of Naval Res., Exp. Towing Tank, Stevens Inst. Tech.), June 1948.
7. Wagner, Herbert: Landing of Seaplanes. NACA TM 622, 1931.
8. Schnitzer, Emanuel: Theory and Procedure for Determining Loads and Motions in Chine-Immersed Hydrodynamic Impacts of Prismatic Bodies. NACA TN 2813, 1952.

TABLE I  
PRESSURE-GAGE POSITIONS  
(See fig. 2)

Gage	$\xi$ (ft)	$\eta$ (ft)	Gage	$\xi$ (ft)	$\eta$ (ft)
1	0.23	0.47	23	1.82	1.08
2	.23	.77	24	1.82	1.24
3	.23	1.08	25	1.82	1.39
4	.23	1.39	26	1.82	1.54
5	.73	.47	27	2.23	.47
6	.73	.77	28	2.23	.77
7	.73	1.08	29	2.57	.47
8	.73	1.39	30	2.57	.77
9	1.02	.62	31	3.40	.32
10	1.07	.47	32	3.40	.47
11	1.07	.77	33	3.40	.62
12	1.07	1.08	34	3.40	.77
13	1.07	1.39	35	.73	-.47
14	1.17	.62	36	.73	-.62
15	1.48	.47	37	.73	-.77
16	1.48	.77	38	.73	-.93
17	1.48	1.08	39	1.07	-.32
18	1.82	.32	40	1.07	-.93
19	1.82	.47	41	1.48	-.32
20	1.82	.62	42	1.48	-.47
21	1.82	.77	43	1.48	-.77
22	1.82	.93			

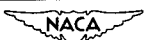


TABLE II  
INITIAL LANDING CONDITIONS AND OVER-ALL LOADS AND MOTIONS

Run	$\tau$ (deg)	At contact				At $(n_{i_w})_{\max}$			At $y_{\max}$		Time, $t$ , at exit (sec)
		$v_o$ (fps)	$\dot{y}_o$ (fps)	$\dot{x}_o$ (fps)	$\gamma_o$ (deg)	$t$ (sec)	$n_{i_w}$ (g)	$y$ (ft)	$\dot{y}$ (fps)	$t$ (sec)	
$W = 1177 \text{ lb}; C_A = 0.48$											
1		10.5	10.5	0	90.00	0.022	3.40	0.22	8.9	-----	-----
2	0.2	10.5	10.5	0	90.00	.025	3.42	.25	8.8	-----	-----
3		10.5	10.5	0	90.00	.029	3.30	.28	8.6	-----	-----
4		80.6	10.1	80.0	7.20	0.040	4.81	0.36	6.9	0.116	0.55
5	3.2	57.7	10.7	56.7	10.69	.041	4.41	.39	7.5	.159	.68
6	6.3	58.2	10.5	57.2	10.40	0.050	4.58	0.46	6.5	0.118	0.64
7	9.3	89.3	7.2	89.0	4.62	0.067	3.77	0.40	3.0	0.094	0.43
8		57.5	10.2	56.6	10.22	.058	4.57	.50	5.5	.106	.62
9		80.5	6.9	80.2	4.92	0.078	3.73	0.41	1.8	0.093	0.42
10		79.3	8.7	78.8	6.30	.068	4.84	.46	2.7	.086	.48
11	12.4	80.5	8.9	80.0	6.35	.067	5.15	.48	3.0	.087	.51
12		58.9	10.8	57.9	10.57	.064	4.88	.58	5.3	.105	.68
13		47.9	10.6	46.7	12.79	.066	4.17	.60	5.9	.127	.75
14		47.1	10.5	45.9	12.88	.062	4.08	.57	6.4	.130	.75
15	20.5	39.4	10.5	38.0	15.45	0.076	3.67	0.67	5.3	0.131	0.80
16	30.3	24.7	10.8	22.2	25.94	0.096	2.24	0.91	7.0	0.245	1.34
$W = 2369 \text{ lb}; C_A = 0.97$											
17		12.0	12.0	0	90.00	0.032	2.63	0.35	10.2	-----	-----
18	0.2	12.0	12.0	0	90.00	.031	2.49	.35	10.5	-----	-----
19		83.2	8.0	82.8	5.52	0.072	3.02	0.51	5.0	0.140	0.66
20	6.3	83.5	11.1	82.8	7.64	.055	4.64	.55	7.4	.136	.80
21		63.8	11.1	62.8	10.02	.058	3.92	.57	7.4	.173	.89
22	12.4	82.2	7.8	81.8	5.45	0.086	3.53	0.54	2.9	0.113	0.58
23		46.5	11.0	45.2	13.68	.068	3.13	.68	7.7	.182	1.05
24	15.4	63.5	11.3	62.5	10.25	0.075	4.24	0.72	5.9	0.126	0.86
25		46.8	11.4	45.4	14.10	.078	3.14	.79	7.2	.178	1.10
26		82.2	7.7	81.8	5.38	0.091	4.13	0.53	1.5	0.103	0.54
27	20.5	83.1	10.8	82.4	7.47	.074	5.59	.63	3.6	.096	.67
28		63.9	11.1	62.9	10.01	.081	4.31	.74	5.0	.123	.84
29		42.2	10.9	40.8	14.96	.087	2.88	.84	6.8	.185	1.14
30	30.3	44.2	11.2	42.8	14.66	-----	2.95	-----	-----	-----	0.428



TABLE III  
VERTICAL-VELOCITY TIME HISTORIES

Run	$\dot{y}$ (fps) at time (sec)															
	0.00	0.01	0.02	0.03	0.04	0.05	0.06	0.07	0.08	0.09	0.10	0.11	0.12	0.13	0.14	0.15
1	10.5	10.0	9.1	8.0	7.1	6.4	5.8	5.3	4.9	4.6	4.6	4.6	4.6	4.6	4.6	4.6
2	10.5	10.2	9.4	8.3	7.3	6.5	6.0	5.9	5.4	5.0	4.7	4.5	4.5	4.5	4.5	4.5
3	10.5	10.3	9.6	8.5	7.5	6.7	6.0	5.5	5.2	4.8	4.6	4.6	4.6	4.6	4.6	4.6
4	10.1	10.0	9.4	8.4	7.4	6.9	6.4	6.0	5.4	5.0	4.7	4.6	4.6	4.6	4.6	4.6
5	10.7	10.6	10.0	9.0	8.0	7.7	6.3	5.0	3.9	3.1	2.4	2.4	2.4	2.4	2.4	2.4
6	10.5	10.4	9.4	9.9	9.1	7.9	6.5	5.0	3.8	2.7	1.8	1.8	1.8	1.8	1.8	1.8
7	7.2	7.2	7.0	6.6	5.9	4.9	3.8	2.6	1.4	1.3	1.4	1.4	1.4	1.4	1.4	1.4
8	10.2	10.1	9.7	9.0	8.0	6.7	6.0	5.3	3.8	2.7	1.5	1.5	1.5	1.5	1.5	1.5
9	6.9	6.8	6.7	6.3	5.7	4.9	3.8	2.7	2.3	1.5	1.4	1.4	1.4	1.4	1.4	1.4
10	8.7	8.6	8.3	7.7	6.7	5.4	4.9	3.9	2.9	2.3	1.8	1.7	1.7	1.7	1.7	1.7
11	8.9	8.8	8.6	8.1	7.1	5.8	4.2	2.6	2.6	1.0	1.4	1.4	1.4	1.4	1.4	1.4
12	10.8	10.7	10.4	9.9	8.9	7.5	6.0	4.4	2.9	1.6	1.6	1.6	1.6	1.6	1.6	1.6
13	10.6	10.5	10.3	9.8	9.0	7.9	6.6	5.3	4.0	2.9	1.9	1.9	1.9	1.9	1.9	1.9
14	10.5	10.4	10.2	9.7	8.9	7.8	6.6	5.3	4.0	2.9	2.0	2.0	2.0	2.0	2.0	2.0
15	10.5	10.4	10.2	9.8	9.1	8.2	7.2	6.0	4.8	3.7	2.6	2.6	2.6	2.6	2.6	2.6
16	10.8	10.8	10.7	10.5	10.2	9.8	9.3	8.7	8.1	7.4	6.7	6.7	6.7	6.7	6.7	6.7
17	12.0	11.8	11.2	10.6	9.6	8.8	8.3	8.0	7.7	7.4	7.1	7.1	7.1	7.1	7.1	7.1
18	12.0	11.8	11.3	10.6	9.8	9.1	8.5	8.1	7.8	7.5	7.3	7.3	7.3	7.3	7.3	7.3
19	8.0	8.0	8.0	7.8	7.4	6.8	6.0	5.1	4.1	3.2	2.4	2.4	2.4	2.4	2.4	2.4
20	11.1	11.1	10.9	10.9	10.4	9.4	8.1	6.6	5.3	4.0	3.0	2.1	2.1	2.1	2.1	2.1
21	11.1	11.1	10.9	10.9	10.4	9.6	8.4	7.2	6.0	4.9	4.0	3.2	2.6	2.6	2.6	2.6
22	7.8	7.8	7.7	7.4	7.0	6.4	5.6	4.6	3.5	2.4	1.3	1.3	1.3	1.3	1.3	1.3
23	11.0	10.9	10.8	10.5	10.1	9.4	8.5	7.5	6.5	5.5	4.7	3.9	3.9	3.9	3.9	3.9
24	11.3	11.3	11.1	10.7	10.1	9.1	7.9	6.6	5.2	3.9	2.7	2.7	2.7	2.7	2.7	2.7
25	11.4	11.4	11.3	11.0	10.6	9.9	9.0	8.0	7.0	6.0	5.1	4.2	3.4	3.4	3.4	3.4
26	7.7	7.7	7.6	7.3	6.9	6.2	5.3	4.2	3.0	1.7	1.4	1.4	1.4	1.4	1.4	1.4
27	10.8	10.7	10.5	9.9	9.0	7.7	6.1	4.4	2.6	1.9	1.7	1.7	1.7	1.7	1.7	1.7
28	11.1	11.1	10.9	10.9	10.5	9.9	9.0	7.8	6.5	5.1	3.8	3.8	3.8	3.8	3.8	3.8
29	10.9	10.9	10.8	10.7	10.3	9.8	9.1	8.3	7.4	6.5	5.6	5.6	5.6	5.6	5.6	5.6
30	11.2	—	—	—	—	—	—	—	—	—	—	—	—	—	—	—



TABLE IV  
INITIAL LANDING CONDITIONS AND MAXIMUM BOTTOM PRESSURES

Run	$\tau$ (deg)	$V_0$ (fps)	$\gamma_0$ (deg)	$\dot{x}_0$ (fps)	Maximum pressure (lb/sq in.) at gage number -																						
					1	2	3	4	5	6	7	8	9	10	11	12	13	14	15	16	17	18	19	20			
1	2	10.5	90.00	10.5	0	6.7	5.9	—	1.1	5.5	5.3	4.0	7.0	5.8	—	3.9	8.7	8.9	5.8	—	6.5	6.7	6.8	6.3			
2	0.2	10.5	90.00	10.5	0	6.9	6.1	—	1.2	6.1	5.4	5.3	6.8	7.5	5.5	—	1.3	8.5	10.2	5.9	—	9.9	6.2	6.6	5.5		
3	10.5	90.00	10.5	0	6.3	6.0	—	1.6	5.1	6.1	5.6	3.9	6.7	6.0	—	4.3	9.1	—	6.5	—	10.4	5.2	7.7	6.0			
4	3.2	80.6	7.20	10.1	80.0	10.1	15.5	—	4.3	10.9	11.2	12.3	7.1	15.1	11.2	—	—	9.1	—	6.5	—	—	—	—	—		
5	57.7	10.69	10.7	56.7	11.5	12.1	—	3.2	8.8	10.4	10.1	15.1	12.0	12.2	8.3	—	—	11.0	12.6	9.7	—	6.3	10.3	11.7	12.2		
6	6.3	58.2	10.40	10.5	57.2	16.0	17.4	—	—	12.7	—	15.3	9.3	16.9	17.0	12.5	—	—	19.6	15.8	12.9	—	12.0	15.2	15.8	12.5	
7	9.3	89.3	1.62	7.2	89.0	22.2	20.3	15.7	—	2.5	19.7	20.1	12.4	0	21.4	32.8	—	—	21.5	25.4	0	0	11.7	10.3	0	0	
8	57.5	10.22	10.2	56.6	—	15.7	—	3.4	17.0	18.5	15.5	—	18.8	27.6	—	—	11.5	18.8	28.6	17.9	—	18.5	13.1	13.8	16.0		
9	80.5	4.92	6.9	80.2	23.1	21.9	—	6.5	—	21.1	10.3	0	21.8	34.9	—	—	0	19.5	21.8	0	—	—	0	—	0		
10	79.3	6.30	8.7	78.8	26.3	24.5	—	2.5	22.8	23.1	19.7	2.2	25.6	38.5	—	—	0	19.5	21.8	0	—	23.6	14.4	0	0		
11	12.4	80.5	6.35	8.9	80.0	27.3	26.3	—	8.2	26.2	25.2	20.6	—	25.9	41.8	23.4	—	1.1	35.2	28.3	9.5	—	29.8	14.5	0	0	
12	47.9	10.57	10.8	57.9	21.9	19.9	—	8.3	21.6	21.9	19.0	17.3	21.4	34.7	19.1	—	13.1	22.1	26.5	19.5	—	25.8	17.9	35.4	17.7		
13	47.1	12.19	12.19	10.6	46.7	18.0	15.1	—	5.3	15.4	16.1	14.3	11.6	20.5	27.1	15.8	—	10.5	17.3	19.7	11.8	—	23.1	13.4	25.3	14.2	
14	39.4	15.45	10.5	38.0	10.5	15.9	14.2	14.4	—	13.3	16.7	17.1	15.5	11.8	16.6	24.9	—	—	10.9	17.4	21.8	15.0	—	21.7	11.9	21.1	11.9
15	20.5	30.3	24.7	25.29	10.6	22.2	8.8	8.2	—	3.8	12.2	11.2	11.6	10.3	15.2	15.6	—	—	11.0	17.1	21.6	2.2	10.2	15.9	10.8	11.8	10.4
16	12.0	90.00	12.0	0	8.9	6.5	—	2.1	6.2	8.2	7.2	5.2	8.3	8.7	—	—	6.0	11.0	13.7	9.0	12.3	9.0	5.6	10.6	9.9	8.9	
17	0.2	12.0	90.00	12.0	0	8.1	7.2	—	2.1	7.1	8.2	7.7	4.5	6.6	8.1	—	—	6.4	10.9	11.0	8.9	—	9.4	3.3	10.0	9.0	8.7
18	19	83.2	5.52	8.0	82.8	15.5	14.6	12.0	6.3	11.6	11.5	11.6	11.1	15.7	25.3	—	—	12.2	16.5	22.7	18.5	13.2	25.6	11.9	17.1	17.9	16.1
20	6.3	83.5	7.61	11.1	82.8	22.5	19.6	—	9.4	21.7	23.2	22.6	17.1	24.7	35.3	—	—	19.1	25.5	25.5	25.0	26.1	27.2	17.0	23.3	26.0	23.8
21	63.8	10.02	11.1	62.8	16.4	15.3	—	6.4	15.9	18.5	17.4	16.5	19.2	28.6	—	—	25.1	18.5	25.4	20.5	16.1	20.5	11.8	17.7	20.4	17.9	
22	82.2	5.45	7.8	81.8	23.6	23.4	10.7	23.9	28.8	24.7	19.9	28.2	13.6	—	—	11.4	20.0	30.8	25.9	0	21.7	20.1	23.6	19.6	2.0		
23	12.4	46.5	13.68	11.0	45.2	16.0	16.1	—	6.3	35.9	18.5	18.5	18.2	14.7	19.7	26.8	—	—	15.4	21.1	25.0	18.9	—	27.8	13.1	16.9	16.1
24	63.5	10.25	11.3	62.5	28.6	26.2	23.1	14.1	24.7	—	29.6	21.7	32.8	15.7	30.5	—	—	20.6	31.1	—	21.8	15.4	—	37.0	22.8	31.3	26.8
25	15.4	46.8	16.10	11.4	45.4	18.4	17.9	11.2	15.5	16.2	17.8	19.7	16.7	21.8	28.1	18.6	—	16.8	29.5	—	21.8	15.4	—	19.1	17.7	—	—
26	82.2	5.38	7.47	10.8	82.4	13.1	37.8	—	13.6	32.2	35.9	31.7	21.4	35.6	51.6	31.4	—	29.1	45.0	16.1	37.3	39.0	26.5	26.4	25.3	10.5	2.1
27	20.5	63.9	10.01	11.1	62.9	26.9	25.4	—	10.7	26.2	31.1	28.2	22.5	29.5	13.1	12.9	—	23.3	32.2	35.0	28.4	—	19.7	21.4	24.5	21.7	—
28	42.2	11.96	10.9	10.8	14.8	14.1	—	7.2	15.1	17.6	17.4	16.0	17.0	25.7	—	—	13.8	18.4	19.7	16.4	—	31.1	10.7	15.6	15.8	14.7	
29	30.3	14.68	11.2	62.8	15.2	19.4	15.8	12.6	16.8	—	22.1	15.6	18.4	18.9	16.4	—	16.6	22.5	—	14.6	—	25.9	12.8	15.7	17.0	16.2	

NACA

**INITIAL LANDING CONDITIONS AND MAXIMUM BOTTOM PRESSURES - Concluded**

Run	$\tau$ (deg)	$V$ (fps)	$\gamma_0$ (deg)	$\dot{\gamma}_0$ (fps)	$\ddot{\gamma}_0$ (fps)	Maximum pressure (lb/sq in.) at gage number—																						
						23	24	25	26	27	28	29	30	31	32	33	34	35	36	37								
1	10.5	90.00	10.5	0	5.2	4.7	4.4	3.4	—	—	7.3	7.7	7.4	7.2	6.2	7.3	5.0	—	6.2	7.4	7.1	—	5.6					
2	0.2	10.5	90.00	10.5	0	5.3	4.6	4.2	3.1	—	6.9	7.6	8.0	7.1	5.9	6.2	5.3	—	3.8	7.3	7.5	—	5.5					
3	10.5	90.00	10.5	0	6.6	4.6	4.9	—	8.0	—	6.9	8.0	7.5	6.8	6.2	6.8	5.7	6.5	1.1	7.4	6.3	6.8	9.5					
4	80.6	7.20	10.1	80.0	10.6	8.7	5.8	—	—	11.2	9.0	12.6	9.5	11.6	6.9	13.1	11.7	16.1	11.5	13.1	11.1	—	5.1					
5	3.2	57.7	10.69	10.7	56.7	8.9	7.9	6.3	—	—	19.0	9.6	12.5	9.5	—	8.6	11.9	9.9	9.6	6.9	13.8	10.7	11.8	0				
6	6.3	58.2	10.40	10.5	57.2	11.3	9.8	8.0	—	15.4	—	13.2	10.4	13.3	10.6	—	7.4	17.1	13.4	14.0	11.0	18.1	13.5	17.1	12.1			
7	9.3	89.3	4.62	7.2	89.0	0	0	—	—	0	0	0	0	0	0	0	24.8	23.2	14.5	15.3	31.3	13.2	23.6	23.9	1.5			
8	57.7	10.22	10.2	56.6	12.0	8.8	6.0	—	17.2	—	11.5	11.1	10.8	2.8	0	0	20.7	19.2	17.1	15.5	27.6	16.0	19.7	24.6	15.2			
9	80.5	4.92	6.9	80.2	0	0	—	—	0	0	0	0	0	0	0	0	25.1	22.3	19.3	15.0	32.5	—	23.6	19.7	0			
10	79.3	6.30	8.7	78.8	0	0	—	—	0	0	0	0	0	0	0	0	21.7	25.4	—	11.7	—	19.1	22.8	—	13.4			
11	80.5	6.35	8.9	80.0	0	2.0	1.5	—	—	2.9	—	0	0	0	0	0	30.5	11.2	—	21.4	26.9	20.3	28.1	30.3	11.6			
12	12.4	58.9	10.57	10.8	57.9	9.5	2.9	—	—	—	0	0	0	0	0	0	23.4	32.4	5.1	16.7	30.2	18.3	26.4	—	16.1			
13	17.9	12.79	10.6	14.7	9.1	1.4	—	—	—	—	13.8	—	10.7	7.6	—	0	0	19.3	—	—	13.0	21.9	16.0	20.5	—	13.2		
14	17.1	12.88	10.5	10.5	45.9	9.5	8.1	6.0	—	—	16.6	—	8.9	9.8	0	0	0	16.7	16.9	—	11.7	22.2	19.2	19.2	—	13.9		
15	20.5	39.4	15.45	10.5	38.0	7.8	5.2	1.9	—	—	8.2	—	8.8	0	0	0	0	15.6	15.1	—	12.0	16.9	13.3	15.8	17.1	10.5		
16	30.3	26.7	2594	10.8	22.2	6.2	4.2	4.7	—	—	5.3	—	3.6	—	0	0	0	8.6	7.7	—	6.3	10.8	6.9	7.2	9.4	6.8		
17	12.0	0.2	90.00	12.0	0	7.9	6.6	7.2	—	—	9.7	—	8.4	12.5	9.7	7.5	9.1	8.0	9.2	8.6	8.5	6.9	9.3	9.4	9.1	—	7.1	
18	12.0	90.00	12.0	0	7.9	6.6	7.0	6.2	—	—	7.0	11.8	9.6	7.2	8.6	7.8	8.4	8.0	7.7	6.9	8.7	8.8	8.3	—	6.6			
19	83.2	5.52	8.0	82.8	13.7	—	—	—	—	—	26.5	44.6	13.0	16.9	12.7	26.2	8.9	16.3	16.4	6.1	12.6	23.6	—	18.4	—	14.1		
20	6.3	83.5	7.64	11.1	82.8	21.2	19.8	17.7	—	—	23.3	—	20.1	22.7	25.0	20.3	19.0	16.3	23.1	23.5	9.7	23.0	31.1	—	19.7	—	14.1	
21	63.8	10.02	11.1	62.8	16.5	15.5	14.4	—	—	20.0	—	15.8	—	20.7	17.2	15.6	15.2	18.3	18.0	5.7	13.9	26.5	17.2	24.0	24.3	20.0	—	14.2
22	82.2	5.45	7.0	81.8	0	2.8	1.3	—	—	17.6	—	15.5	0	0	0	0	28.8	28.2	—	22.0	39.7	23.4	30.6	—	20.0	—	14.2	
23	12.4	13.68	11.0	45.2	16.2	15.3	—	—	—	—	18.9	0	15.5	19.2	15.6	13.1	11.9	10.6	19.7	19.0	—	16.5	26.7	21.7	21.7	—	14.2	
24	63.5	10.25	11.3	62.5	22.5	21.1	17.5	—	—	27.0	—	13.5	21.0	0	0	0	0	15.6	15.1	—	25.8	25.6	25.8	25.8	22.7	—	22.7	
25	15.4	46.8	14.10	11.4	45.4	18.1	16.6	13.8	—	—	20.0	—	10.5	18.1	13.7	11.5	10.0	6.8	11.2	19.1	—	15.9	25.5	21.7	22.8	—	17.1	
26	82.2	5.38	7.7	81.8	0	—	—	—	—	—	0	—	0	0	0	0	0	36.5	36.8	52.6	22.9	16.2	28.6	51.7	32.4	15.2	—	20.7
27	83.1	7.47	10.8	82.4	—	3.7	—	—	—	—	0	—	0	0	0	0	0	44.1	42.4	—	15.9	26.5	25.5	33.1	—	20.7		
28	20.5	63.9	10.01	11.1	62.9	19.6	11.7	8.0	—	—	22.9	—	0	0	0	0	0	33.3	32.9	13.3	26.7	13.6	25.5	33.1	—	20.7		
29	42.2	14.2	14.66	11.2	42.8	15.4	13.4	10.5	—	—	16.2	—	10.8	11.6	0	0	0	0	0	17.8	18.8	7.5	25.7	25.7	25.7	11.6	—	11.6
30	30.3	14.4	26.7	10.8	22.2	6.2	4.2	4.7	—	—	5.3	—	3.6	—	0	0	0	8.6	7.7	—	6.3	10.8	6.9	7.2	9.4	6.8		

TABLE V  
TIMES OF MAXIMUM BOTTOM PRESSURES

Run	Time of maximum pressure (sec) on gage number-																				
	1	2	3	4	5	6	7	8	9	10	11	12	13	14	15	16	17	18	19	20	21
1	0.010	0.019	0.034	0.046	0.008	0.019	0.032	0.045	0.015	0.009	0.019	0.031	0.045	0.016	0.011	0.021	0.032	0.013	0.017	0.022	0.027
2	0.011	0.021	0.033	0.046	0.012	0.020	0.032	0.044	0.013	0.011	0.020	0.031	0.043	0.015	0.011	0.022	0.033	0.008	0.013	0.017	0.023
3	0.012	0.021	0.034	0.047	0.010	0.020	0.034	0.046	0.016	0.011	0.020	0.032	0.046	0.017	0.012	0.023	0.034	0.009	0.015	0.017	0.025
4	0.010	0.020	0.033	0.047	0.013	0.021	0.035	0.047	0.016	0.010	0.020	0.034	0.047	0.017	0.012	0.020	0.030	0.020	0.023	0.030	0.028
5	0.012	0.020	0.033	0.045	0.015	0.026	0.035	0.046	0.020	0.016	0.026	0.037	0.047	0.021	0.016	0.025	0.030	0.018	0.023	0.027	0.035
6	0.013	0.023	0.034	0.044	0.016	0.026	0.037	0.047	0.021	0.016	0.026	0.032	0.042	0.026	0.021	0.027	0.035	0.025	0.027	0.033	0.037
7	0.020	0.036	0.054	0.090	0.033	0.049	0.083	0.124	0.024	0.021	0.024	0.032	0.042	0.026	0.021	0.027	0.035	0.025	0.032	0.036	0.043
8	0.021	0.032	0.045	0.081	0.018	0.028	0.040	0.055	0.028	0.025	0.035	0.048	0.063	0.032	0.032	0.045	0.058	(a)	0.061	0.080	(a)
9	0.021	0.039	0.056	0.090	—	0.055	0.094	(a)	0.060	0.053	0.080	—	(a)	0.071	0.094	(a)	—	0.038	0.050	0.047	0.052
10	0.018	0.029	0.043	0.070	0.032	0.043	0.060	0.094	0.032	0.030	0.043	0.064	0.095	0.037	0.041	0.064	0.083	(a)	(a)	(a)	(a)
11	0.018	0.028	0.042	0.059	0.029	0.042	0.058	0.088	0.044	0.041	0.039	0.054	0.087	0.049	0.054	0.085	0.083	(a)	(a)	(a)	(a)
12	0.014	0.024	0.034	0.046	0.024	0.034	0.044	0.059	0.031	0.031	0.031	0.041	0.054	0.070	0.037	0.041	0.054	0.063	0.083	(a)	(a)
13	0.014	0.024	0.031	0.045	0.023	0.033	0.043	0.056	0.033	0.031	0.031	0.040	0.051	0.070	0.037	0.041	0.054	0.063	0.083	(a)	(a)
14	0.017	0.026	0.037	0.047	0.026	0.035	0.046	0.058	0.036	0.032	0.042	0.058	0.070	0.038	0.040	0.053	0.064	0.069	0.081	0.091	0.075
15	0.017	0.026	0.035	0.046	0.028	0.038	0.048	0.062	0.042	0.039	0.042	0.059	0.071	0.062	0.077	0.087	0.078	0.087	0.091	0.098	0.106
16	0.018	0.027	0.038	0.048	0.039	0.045	0.055	0.067	0.051	0.052	0.061	0.072	0.081	0.072	0.082	0.092	0.087	0.097	0.107	0.115	0.124
17	0.010	0.018	—	—	0.012	0.009	0.019	0.028	0.019	0.011	0.010	0.028	0.039	0.051	0.010	0.011	0.020	0.008	0.013	0.017	0.022
18	0.011	0.019	—	—	0.012	0.010	0.019	0.030	0.019	0.015	0.011	0.028	0.040	0.016	0.012	0.021	0.029	0.007	0.013	0.016	0.026
19	0.020	0.033	0.047	0.061	0.028	0.040	0.053	0.068	0.038	0.031	0.040	0.058	0.078	0.040	0.040	0.053	0.064	0.066	0.084	0.094	0.071
20	0.014	0.024	0.034	0.047	0.011	0.020	0.028	0.036	0.018	0.025	0.024	0.032	0.044	0.053	0.027	0.026	0.036	0.047	0.058	0.071	0.083
21	0.013	0.021	0.032	0.041	0.016	0.026	0.036	0.046	0.020	0.026	0.020	0.039	0.050	0.026	0.026	0.036	0.042	0.036	0.046	0.052	0.065
22	0.021	0.034	0.048	0.064	0.034	0.048	0.063	0.085	0.050	0.048	0.059	0.079	0.110	0.055	0.060	0.077	—	0.066	0.071	0.080	0.097
23	0.012	0.020	0.031	0.040	0.020	0.030	0.040	0.050	0.030	0.028	0.033	0.040	0.057	0.035	0.036	0.045	—	0.040	0.051	0.054	0.060
24	0.015	0.024	0.032	0.040	0.025	0.032	0.042	0.053	0.035	0.033	0.040	0.053	0.063	0.040	0.040	0.053	0.063	0.069	0.080	0.091	0.071
25	0.014	0.023	0.034	0.042	0.024	0.033	0.041	0.052	0.034	0.032	0.041	0.051	0.061	0.039	0.041	0.052	0.060	0.066	0.072	0.087	0.096
26	0.024	0.034	0.048	0.064	0.034	0.048	0.064	0.075	0.055	0.059	0.075	0.104	0.071	0.074	0.099	0.126	(a)	(a)	—	—	—
27	0.014	0.022	0.032	0.042	0.012	0.029	0.037	0.047	0.059	0.042	0.040	0.048	0.077	0.048	0.056	0.068	0.077	0.071	0.087	0.092	0.097
28	0.013	0.023	0.032	0.042	0.028	0.036	0.046	0.056	0.041	0.038	0.047	0.056	0.070	0.046	0.052	0.062	0.067	0.072	0.079	0.087	0.096
29	0.010	0.020	0.030	0.040	0.025	0.032	0.040	0.053	0.036	0.035	0.043	0.050	0.065	0.043	0.050	0.060	0.067	0.061	0.067	0.074	0.080
30	0.017	0.025	0.035	0.042	0.024	0.031	0.039	0.051	0.050	0.050	0.051	0.056	0.075	0.075	0.077	0.087	0.080	0.087	0.092	0.097	0.103

a zero pressure on gage.

NACA

TABLE V - Concluded  
TIME OF MAXIMUM BOTTOM PRESSURES - Concluded

Run	Time of maximum pressure (sec) on gage number -												
	23	24	25	26	27	28	29	30	31	32	33	34	35
1	0.035	0.040	0.047	0.055	-----	-----	0.016	0.026	0.012	0.017	0.022	0.026	0.017
2	.033	.040	.045	.051	-----	-----	.013	.026	.012	.017	.022	.027	.015
3	.035	.040	.047	-----	.017	-----	.017	.026	.014	.018	.024	.027	.017
4	.049	.058	.070	-----	.028	-----	.030	.042	.032	.036	.042	.025	.026
5	.045	.052	.059	-----	.026	-----	.032	.041	.028	.034	.040	.021	.017
6	.056	-----	.075	-----	.039	-----	.014	.056	.056	.047	.056	.025	.028
7	(a)	(a)	(a)	(a)	(a)	-----	(a)	(a)	(a)	(a)	(a)	.054	.064
8	.068	(a)	.108	-----	.049	-----	.059	.080	.082	.108	(a)	.038	.040
9	(a)	(a)	(a)	(a)	(a)	-----	(a)	(a)	(a)	(a)	(a)	.026	.030
10	(a)	(a)	(a)	(a)	(a)	-----	(a)	(a)	(a)	(a)	(a)	.014	.014
11	(a)	.088	.093	-----	.068	-----	(a)	(a)	(a)	(a)	(a)	.035	.051
12	.094	.054	-----	-----	.066	-----	.089	(a)	(a)	(a)	(a)	.036	.040
13	.078	.090	.110	-----	.063	-----	.077	.103	(a)	(a)	(a)	.030	.034
14	.082	.092	.107	-----	.065	-----	.077	.100	(a)	(a)	(a)	.029	.033
15	.107	.127	.137	-----	.102	-----	(a)	(a)	(a)	(a)	(a)	.038	.038
16	.115	.121	.131	-----	.126	-----	.161	-----	(a)	(a)	(a)	.036	.041
17	.030	.036	.042	-----	.015	-----	.026	.010	.016	.020	.025	.017	.050
18	.031	.032	.042	-----	.015	-----	.015	.026	.012	.016	.026	.016	.024
19	.074	-----	-----	-----	.051	-----	.058	.074	.064	.074	.086	.032	.039
20	.052	.057	.065	-----	.036	-----	.042	.053	.045	.052	.056	.025	.031
21	.051	.056	.061	-----	.036	-----	.040	-----	.014	.016	.021	.026	.030
22	(a)	.074	-----	-----	.110	-----	.085	(a)	(a)	(a)	.023	.027	.033
23	.065	.070	.076	-----	.054	-----	.063	.076	.082	.089	.095	.045	.058
24	.078	.088	.097	-----	.069	-----	.083	.112	(a)	(a)	(a)	.027	.031
25	.071	.077	.084	-----	.064	-----	.075	.093	.112	.122	.136	.034	.048
26	(a)	.069	(a)	-----	(a)	-----	.098	(a)	(a)	(a)	(a)	.019	.056
27	-----	(a)	-----	-----	(a)	-----	(a)	(a)	(a)	(a)	(a)	.035	.039
28	.097	.112	.119	-----	.092	-----	(a)	(a)	(a)	(a)	(a)	.033	.037
29	.090	.098	(a)	-----	.085	-----	.105	.115	.179	(a)	(a)	.035	.042
30	.110	.118	.122	-----	.120	-----	-----	-----	-----	-----	-----	.045	.051

a zero pressure on gage.



TABLE VI  
INSTANTANEOUS PRESSURE DISTRIBUTIONS

(a)  $W = 1177 \text{ lb}; C_d = 0.48$ 

Run	$\tau$ (deg)	$t$ (sec)	$y$ (ft)	$\dot{y}$ (ft/sec)	$n_1$ (g)	Pressure (lb/sq in.) at gauge number -																			
						1	2	3	4	5	6	7	8	9	10	11	12	13	14	15	16	17			
1	0.2	0.027	0.26	8.4	3.28	1.6	2.9	—	0	1.5	2.8	0.5	0	2.0	2.3	2.0	3.4	2.0	3.3	—	4.0	2.9	4.2	6.3	
		0.030	.36	7.2	2.62	1.0	2.1	—	0	1.2	1.5	2.6	1.1	0.6	1.4	1.5	0	1.6	2.0	1.4	1.6	1.7	3.5	2.1	
	0.2	0.070	.47	6.0	1.85	1.0	1.7	—	0	1.2	1.1	1.0	1.1	1.1	1.1	1.1	1.1	1.1	1.1	1.2	1.2	1.2	1.7		
		0.070	.55	5.3	1.20	1.0	1.7	—	0	1.1	1.1	1.1	1.1	1.1	1.1	1.1	1.1	1.1	1.1	1.2	1.2	1.2	1.7		
2	0.2	0.027	0.26	8.6	3.35	1.4	2.6	—	0	2.0	2.3	0.5	—	1.4	1.7	2.2	0	2.9	1.6	3.2	3.2	3.2	3.5	2.5	
		0.030	.37	7.3	2.65	1.2	1.3	—	0	1.5	1.3	2.5	—	0.9	0.7	1.0	1.1	1.1	1.1	1.1	1.1	1.1	1.1	1.1	1.5
	0.2	0.070	.51	6.2	1.95	1.5	1.7	—	0	1.5	1.5	1.5	1.5	1.5	1.5	1.5	1.5	1.5	1.5	1.5	1.5	1.5	1.5		
		0.070	.55	5.4	1.25	1.3	1.3	—	0	1.5	1.4	1.4	1.4	1.4	1.4	1.4	1.4	1.4	1.4	1.4	1.4	1.4	1.4		
3	0.2	0.028	0.28	8.7	3.30	1.3	2.6	—	0	1.3	2.7	0	0	1.3	1.8	2.8	—	0	3.4	—	3.6	—	3.6	—	
		0.030	.48	6.4	1.99	1.0	1.8	—	0	1.1	1.1	1.1	1.1	1.1	1.1	1.1	1.1	1.1	1.1	1.1	1.1	1.1	1.1		
	0.2	0.070	.57	5.6	1.30	1.0	1.4	—	0	1.1	1.1	1.1	1.1	1.1	1.1	1.1	1.1	1.1	1.1	1.1	1.1	1.1	1.1		
		0.070	.60	4.5	4.53	1.8	3.9	—	0	1.4	1.4	1.4	1.4	1.4	1.4	1.4	1.4	1.4	1.4	1.4	1.4	1.4	1.4		
4	0.2	0.030	0.42	5.4	3.26	1.5	2.8	—	0	1.6	1.6	1.6	1.6	1.6	1.6	1.6	1.6	1.6	1.6	1.6	1.6	1.6	1.6		
		0.030	.50	2.8	3.26	1.5	2.8	—	0	1.4	1.4	1.4	1.4	1.4	1.4	1.4	1.4	1.4	1.4	1.4	1.4	1.4	1.4		
	0.2	0.070	.63	4.07	3.0	4.9	—	0	1.4	1.4	1.4	1.4	1.4	1.4	1.4	1.4	1.4	1.4	1.4	1.4	1.4	1.4	1.4		
		0.070	.65	4.2	6.9	3.8	3.0	—	0	1.2	1.2	1.2	1.2	1.2	1.2	1.2	1.2	1.2	1.2	1.2	1.2	1.2	1.2		
5	0.2	0.030	0.45	5.9	3.38	2.3	3.2	—	0	1.4	1.4	1.4	1.4	1.4	1.4	1.4	1.4	1.4	1.4	1.4	1.4	1.4	1.4		
		0.030	.50	4.9	3.63	1.0	1.8	—	0	1.4	1.4	1.4	1.4	1.4	1.4	1.4	1.4	1.4	1.4	1.4	1.4	1.4	1.4		
	0.2	0.070	.64	1.7	1.13	1.8	1.8	—	0	1.5	1.5	1.5	1.5	1.5	1.5	1.5	1.5	1.5	1.5	1.5	1.5	1.5	1.5		
		0.070	.65	1.7	4.12	3.4	5.2	—	0	1.6	1.6	1.6	1.6	1.6	1.6	1.6	1.6	1.6	1.6	1.6	1.6	1.6	1.6		
6	0.2	0.030	0.49	5.6	4.47	2.4	3.3	—	0	2.0	2.4	—	8.2	2.9	2.9	2.9	—	5.5	5.0	5.0	5.0	5.0	5.0	5.0	
		0.030	.57	3.4	3.6	2.1	2.7	—	0	1.6	1.6	1.6	1.6	1.6	1.6	1.6	1.6	1.6	1.6	1.6	1.6	1.6	1.6		
	0.2	0.070	.63	1.8	1.87	1.6	2.5	—	0	1.7	1.7	1.7	1.7	1.7	1.7	1.7	1.7	1.7	1.7	1.7	1.7	1.7	1.7		
		0.070	.65	1.8	3.54	4.4	6.3	—	0	1.4	1.4	1.4	1.4	1.4	1.4	1.4	1.4	1.4	1.4	1.4	1.4	1.4	1.4		
7	0.2	0.030	0.43	1.1	3.54	4.4	6.3	—	0	1.4	1.4	1.4	1.4	1.4	1.4	1.4	1.4	1.4	1.4	1.4	1.4	1.4	1.4		
		0.030	.50	8.0	3.63	3.9	—	0	5.9	9.6	15.5	—	8.2	11.4	—	—	—	9.0	12.7	0	0	7.4	10.3	0	
	0.2	0.070	.63	1.1	3.54	4.4	6.3	—	0	1.4	1.4	1.4	1.4	1.4	1.4	1.4	1.4	1.4	1.4	1.4	1.4	1.4	1.4		
		0.070	.65	1.1	3.54	4.4	6.3	—	0	1.4	1.4	1.4	1.4	1.4	1.4	1.4	1.4	1.4	1.4	1.4	1.4	1.4	1.4		
8	0.2	0.030	0.49	5.4	4.47	3.3	3.3	—	0	3.7	4.8	6.1	—	4.1	7.6	—	—	5.5	5.0	5.0	5.0	5.0	5.0	5.0	
		0.030	.55	2.4	3.73	2.6	2.2	—	0	2.1	2.8	—	3.3	8.1	—	—	6.6	2.0	3.2	0	0	6.6	6.6	0	
	0.2	0.070	.65	1.5	3.73	5.6	7.9	—	0	1.4	7.8	10.0	5.1	0	10.8	18.4	—	0	18.8	21.8	0	—	18.8	21.8	0
		0.070	.65	1.5	4.66	5.6	8.5	—	0	3.1	3.1	3.1	9.8	0	15.4	21.6	—	0	19.8	28.8	0	—	19.8	28.8	0
9	0.2	0.030	0.45	5.5	4.47	3.3	3.3	—	0	1.4	1.4	1.4	1.4	1.4	1.4	1.4	1.4	1.4	1.4	1.4	1.4	1.4	1.4		
		0.030	.55	2.4	3.73	5.6	7.9	—	0	1.4	7.8	10.0	5.1	0	10.8	18.4	—	0	18.8	21.8	0	—	18.8	21.8	0
	0.2	0.070	.65	1.5	3.73	5.6	7.9	—	0	1.4	7.8	10.0	5.1	0	10.8	18.4	—	0	18.8	21.8	0	—	18.8	21.8	0
		0.070	.65	1.5	4.66	5.6	8.5	—	0	3.1	3.1	3.1	9.8	0	15.4	21.6	—	0	19.8	28.8	0	—	19.8	28.8	0
10	0.2	0.030	0.45	5.5	4.47	3.3	3.3	—	0	1.4	1.4	1.4	1.4	1.4	1.4	1.4	1.4	1.4	1.4	1.4	1.4	1.4	1.4		
		0.030	.55	2.4	3.73	5.6	7.9	—	0	1.4	7.8	10.0	5.1	0	10.8	18.4	—	0	18.8	21.8	0	—	18.8	21.8	0
	0.2	0.070	.65	1.5	3.73	5.6	7.9	—	0	1.4	7.8	10.0	5.1	0	10.8	18.4	—	0	18.8	21.8	0	—	18.8	21.8	0
		0.070	.65	1.5	4.66	5.6	8.5	—	0	3.1	3.1	3.1	9.8	0	15.4	21.6	—	0	19.8	28.8	0	—	19.8	28.8	0
11	0.2	0.030	0.45	5.5	4.47	3.3	3.3	—	0	1.4	1.4	1.4	1.4	1.4	1.4	1.4	1.4	1.4	1.4	1.4	1.4	1.4	1.4		
		0.030	.55	2.4	3.73	5.6	7.9	—	0	1.4	7.8	10.0	5.1	0	10.8	18.4	—	0	18.8	21.8	0	—	18.8	21.8	0
	0.2	0.070	.65	1.5	3.73	5.6	7.9	—	0	1.4	7.8	10.0	5.1	0	10.8	18.4	—	0	18.8	21.8	0	—	18.8	21.8	0
		0.070	.65	1.5	4.66	5.6	8.5	—	0	3.1	3.1	3.1	9.8	0	15.4	21.6	—	0	19.8	28.8	0	—	19.8	28.8	0
12	0.2	0.030	0.45	5.5	4.47	3.3	3.3	—	0	1.4	1.4	1.4	1.4	1.4	1.4	1.4	1.4	1.4	1.4	1.4	1.4	1.4	1.4		
		0.030	.55	2.4	3.73	5.6	7.9	—	0	1.4	7.8	10.0	5.1	0	10.8	18.4	—	0	18.8	21.8	0	—	18.8	21.8	0
	0.2	0.070	.65	1.5	3.73	5.6	7.9	—	0	1.4	7.8	10.0	5.1	0	10.8	18.4	—	0	18.8	21.8	0	—	18.8	21.8	0
		0.070	.65	1.5	4.66	5.6	8.5	—	0	3.1	3.1	3.1	9.8	0	15.4	21.6	—	0	19.8	28.8	0	—	19.8	28.8	0
13	0.2	0.030	0.45	5.5	4.47	3.3	3.3	—	0	1.4	1.4	1.4	1.4	1.4	1.4	1.4	1.4	1.4	1.4	1.4	1.4	1.4	1.4		
		0.030	.55	2.4	3.73	5.6	7.9	—	0	1.4	7.8	10.0	5.1	0	10.8	18.4	—	0	18.8	21.8	0	—	18.8	21.8	0

TABLE VI - Continued  
INSTANTANEOUS PRESSURE DISTRIBUTIONS - Continued  
(a) Continued

TABLE VI - Continued  
INSTANTANEOUS PRESSURE DISTRIBUTIONS - Continued

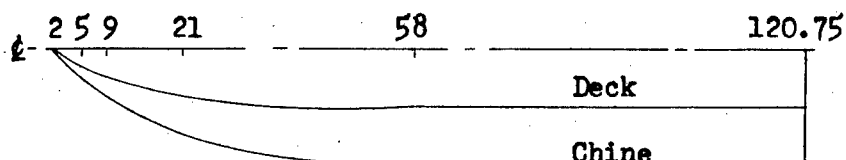


TABLE VI - Concluded  
INSTANTANEOUS PRESSURE DISTRIBUTIONS - Concluded

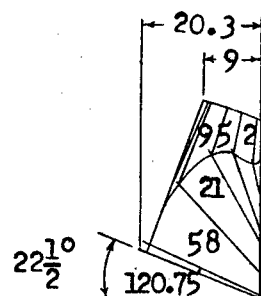
## (b) Concluded

Run	$\tau$ (deg)	t (sec)	x (ft)	y (fps)	z (g)	Pressure (lb/sq in.) at gage number -																										
						23	24	25	26	27	28	29	30	31	32	33	34	35	36	37	38											
17	0.2	0.026	0.29	10.7	2.51	-0.5	-0.2	0.9	---	5.1	---	4.3	10.6	3.9	3.8	5.2	7.2	3.7	4.0	6.4	0.6	3.3	2.1	3.8	---	4.3						
		0.036	.40	9.8	2.58	4.7	6.6	1.1	3.2	3.3	---	2.7	4.4	2.3	2.7	3.0	3.5	2.3	2.6	3.0	3.5	1.7	3.0	2.3	1.5	2.2						
		0.051	.57	8.6	1.75	1.4	1.4	1.4	1.8	1.8	---	2.2	2.2	1.6	1.5	1.7	1.2	1.7	1.7	1.0	1.0	1.7	1.0	1.6	1.5	1.5	.9					
18	0.2	0.026	0.30	10.9	2.49	-0.9	0	0	---	3.8	---	3.0	11.8	3.7	5.2	7.8	3.4	3.9	7.9	5.6	3.0	0.6	3.0	2.3	5.7	2.3	2.3	3.8				
		0.032	.36	10.4	2.49	-7.9	7.0	2.4	---	2.8	---	2.4	5.8	2.6	3.0	3.3	4.5	2.7	3.0	3.0	3.0	3.0	0.6	2.3	5.7	2.3	2.3					
		0.051	.57	8.8	1.82	1.2	1.6	2.4	0	1.5	---	1.2	1.8	0.7	1.1	0.8	1.2	0.9	1.0	1.3	0.7	.8	1.1	0.7	1.1	1.1	1.1	.3				
19	6.3	0.074	.52	6.2	2.61	2.5	0	0	---	11.3	37.2	13.2	0	0	0	0	6.1	6.4	2.7	10.4	7.6	1.1	1.1	1.1	1.1	1.1	1.1	1.1	12.1			
		0.110	.63	4.8	4.8	3.01	13.7	1.9	---	7.5	45.3	7.2	1.6	11.7	12.7	0	0	3.4	3.6	1.4	5.5	5.1	6.4	6.4	6.4	6.4	6.4	6.4				
20	6.3	0.012	0.44	9.2	3.91	3.7	0	0	---	16.5	---	20.1	0	0	0	0	8.8	10.7	2.0	7	7	2.2	2.5	2.5	2.5	2.5	2.5	2.5	3.5			
		0.065	.62	5.9	4.28	10.6	13.2	17.7	9.0	---	12.0	---	10.0	0	16.5	20.3	1.2	0	6.1	7.1	3.3	19.1	12.8	---	---	---	---	---	17.2			
		0.040	0.42	9.5	3.17	0	0	0	0	---	7.5	11.4	11.2	11.1	11.5	16.3	16.1	5.0	0	1.9	5.5	6.0	6.0	6.0	6.0	6.0	6.0	6.0				
21	6.3	0.051	.52	8.3	3.79	16.5	3.8	1.3	---	15.4	---	0	0	0	0	5.4	6.5	3.6	11.7	7.7	11.8	8.3	10.3	13.6	13.6	13.6	13.6	13.6				
		0.062	.60	6.9	3.88	8.2	10.8	13.1	6.2	---	8.5	---	7.6	0	11.3	17.2	0	0	4.1	3.6	2.3	6.7	6.8	7.2	5.0	5.9	7.1	7.1	7.1			
		0.133	.87	1.4	1.34	2.5	1.9	1.3	2.3	---	6.2	---	5.3	0	8.0	8.6	9.8	15.2	2.0	2.2	0	3.9	4.3	4.4	5.0	5.0	5.6	5.6				
22	12.4	0.059	0.42	5.7	2.70	0	0	0	0	---	1.8	0	0	0	0	1.8	0	0	0	0	0	0	0	0	0	0	0	1.5				
		0.095	.54	3.0	3.56	0	2.3	0	0	0	1.5	---	0	0	0	0	0	0	0	0	0	0	0	0	0	0	0	0	2.0			
		0.050	0.53	9.4	2.55	0	2.8	0	0	0	11.6	0	0	0	0	0	0	0	0	0	0	0	0	0	0	0	0	0	0	16.1		
23	12.4	0.060	.62	8.5	3.10	0	2.8	0	0	0	11.6	0	0	0	0	0	0	0	0	0	0	0	0	0	0	0	0	0	0	13.7		
		0.076	.74	6.9	3.15	10.6	12.0	13.5	0	7.3	0	6.5	19.2	0	0	0	0	5.4	5.6	5.6	5.6	5.6	5.6	5.6	5.6	5.6	5.6	5.6				
		0.105	.90	4.2	5.05	3.1	3.7	3.2	0	2.2	0	5.4	6.4	7.1	6.6	7.9	10.6	1.4	2.7	4.2	4.2	4.2	4.2	4.2	4.2	4.2	4.2	4.2				
24	15.4	0.011	0.45	10.0	2.58	0	0	0	0	0	0	0	0	0	0	0	0	0	0	0	0	0	0	0	0	0	0	0	0	1.0		
		0.088	.79	4.2	4.07	20.0	22.0	10.8	---	15.4	---	0	0	0	0	0	0	0	0	0	0	0	0	0	0	0	0	0	0	1.0		
25	15.4	0.041	0.45	10.5	1.80	0	0	0	0	0	0	0	0	0	0	0	0	0	0	0	0	0	0	0	0	0	0	0	0	0	6.6	
		0.077	.78	7.3	3.11	16.1	16.6	3.5	---	12.8	---	9.9	0	0	0	0	0	0	0	0	0	0	0	0	0	0	0	0	0	0		
26	20.5	0.074	0.48	3.8	3.73	0	---	0	0	0	0	0	0	0	0	0	0	0	0	0	0	0	0	0	0	0	0	0	0	0	0	
		0.047	0.47	8.1	4.35	0	3.7	0	0	0	0	0	0	0	0	0	0	0	0	0	0	0	0	0	0	0	0	0	0	0	0	2.0
27	20.5	0.077	.64	3.1	5.56	0	3.7	0	0	0	0	0	0	0	0	0	0	0	0	0	0	0	0	0	0	0	0	0	0	0	0	24.7
		0.016	0.49	9.4	3.04	0	0	0	0	0	0	0	0	0	0	0	0	0	0	0	0	0	0	0	0	0	0	0	0	0	0	0
28	20.5	0.070	.68	6.5	4.16	0	3.2	0	0	0	0	0	0	0	0	0	0	0	0	0	0	0	0	0	0	0	0	0	0	0	0	0
		.097	.81	2.9	3.91	19.6	11.6	0	22.9	0	0	0	0	0	0	0	0	0	0	0	0	0	0	0	0	0	0	0	0	0	0	0
29	20.5	0.042	0.45	10.2	1.46	0	0	0	0	0	0	0	0	0	0	0	0	0	0	0	0	0	0	0	0	0	0	0	0	0	0	0
		0.063	.65	8.9	2.47	0	2.8	0	0	0	0	0	0	0	0	0	0	0	0	0	0	0	0	0	0	0	0	0	0	0	0	0
		0.088	.85	6.7	2.86	12.7	1.6	0	16.2	0	-1.8	0	0	0	0	0	0	0	0	0	0	0	0	0	0	0	0	0	0	0	0	
30	30.3	0.057	1.05	---	---	14.9	11.4	5.6	---	2.2	1.6	0	0	0	0	0	0	0	0	0	0	0	0	0	0	0	0	0	0	0		
		0.057	1.05	---	---	14.9	11.4	5.6	---	0.2	---	0.2	---	0.2	---	0.2	---	0.2	---	0.2	---	0.2	---	0.2	---	0.2	---	0.2	---	0.2	0.2	

NACA



Half-breadth



Body plan

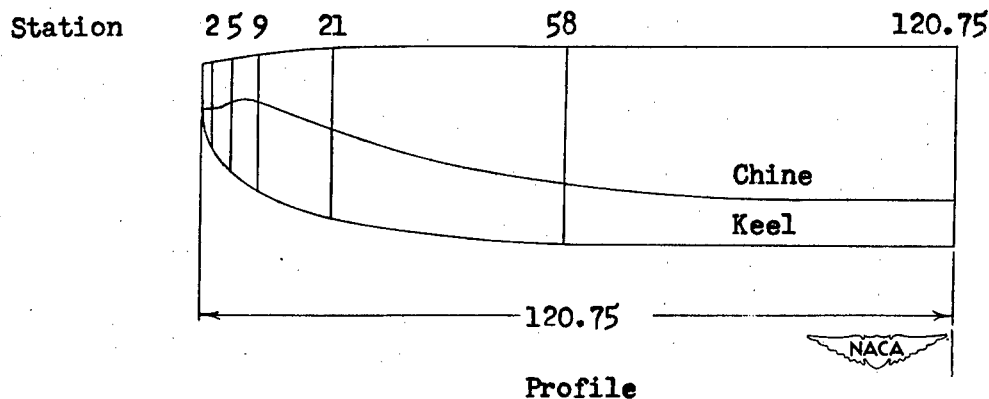


Figure 1.- Hull lines of float having a  $22\frac{1}{2}^{\circ}$  angle of dead rise.  
(All dimensions are in inches.)

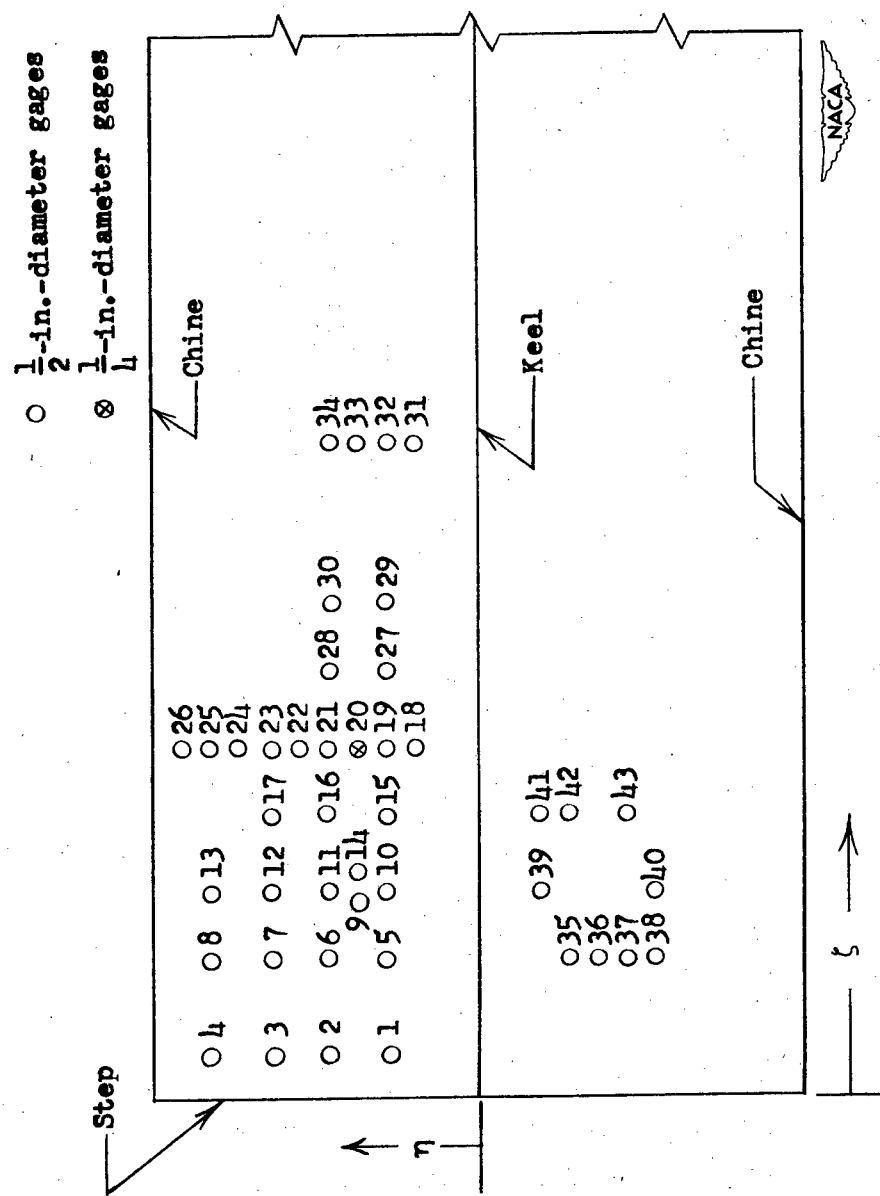


Figure 2.- Location of pressure gages in float bottom.

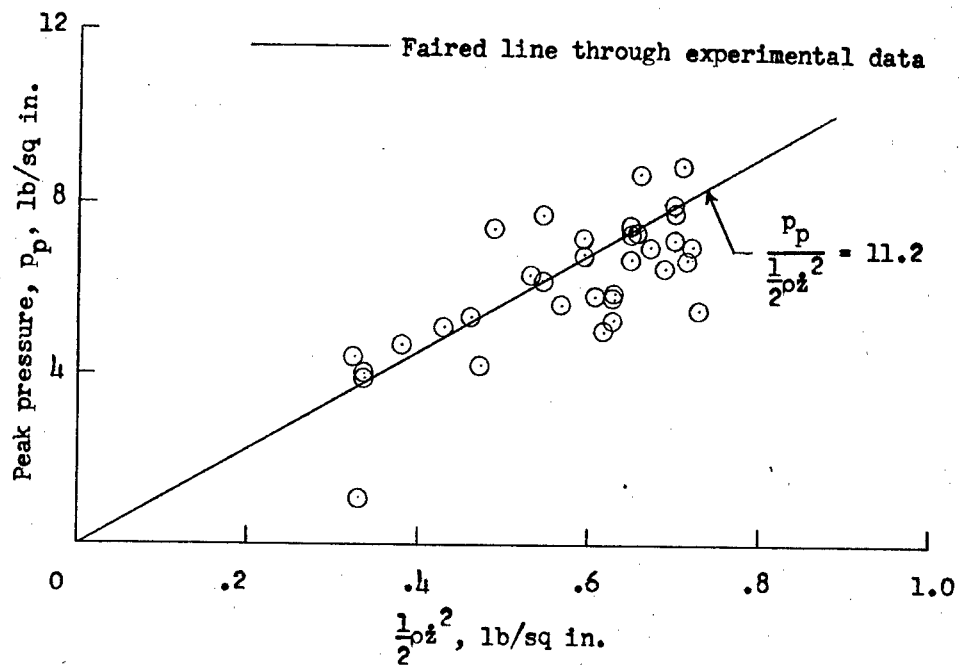
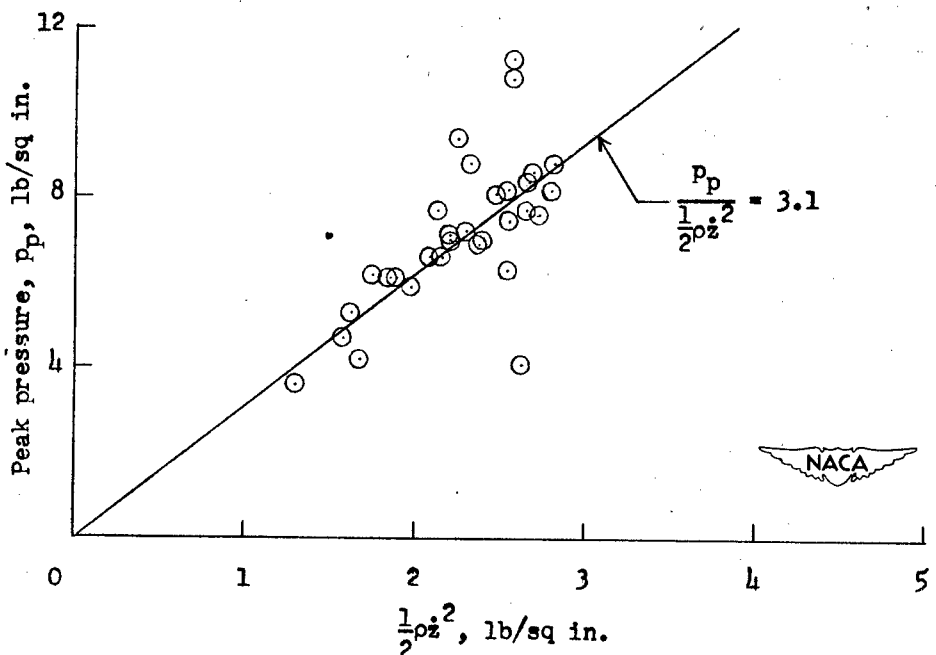
(a) Run 1;  $\tau = 0.2^\circ$ .(b) Run 16;  $\tau = 30.3^\circ$ .

Figure 3.- Experimental variation of the peak pressure with  $\frac{1}{2}\rho z^2$  for two runs.

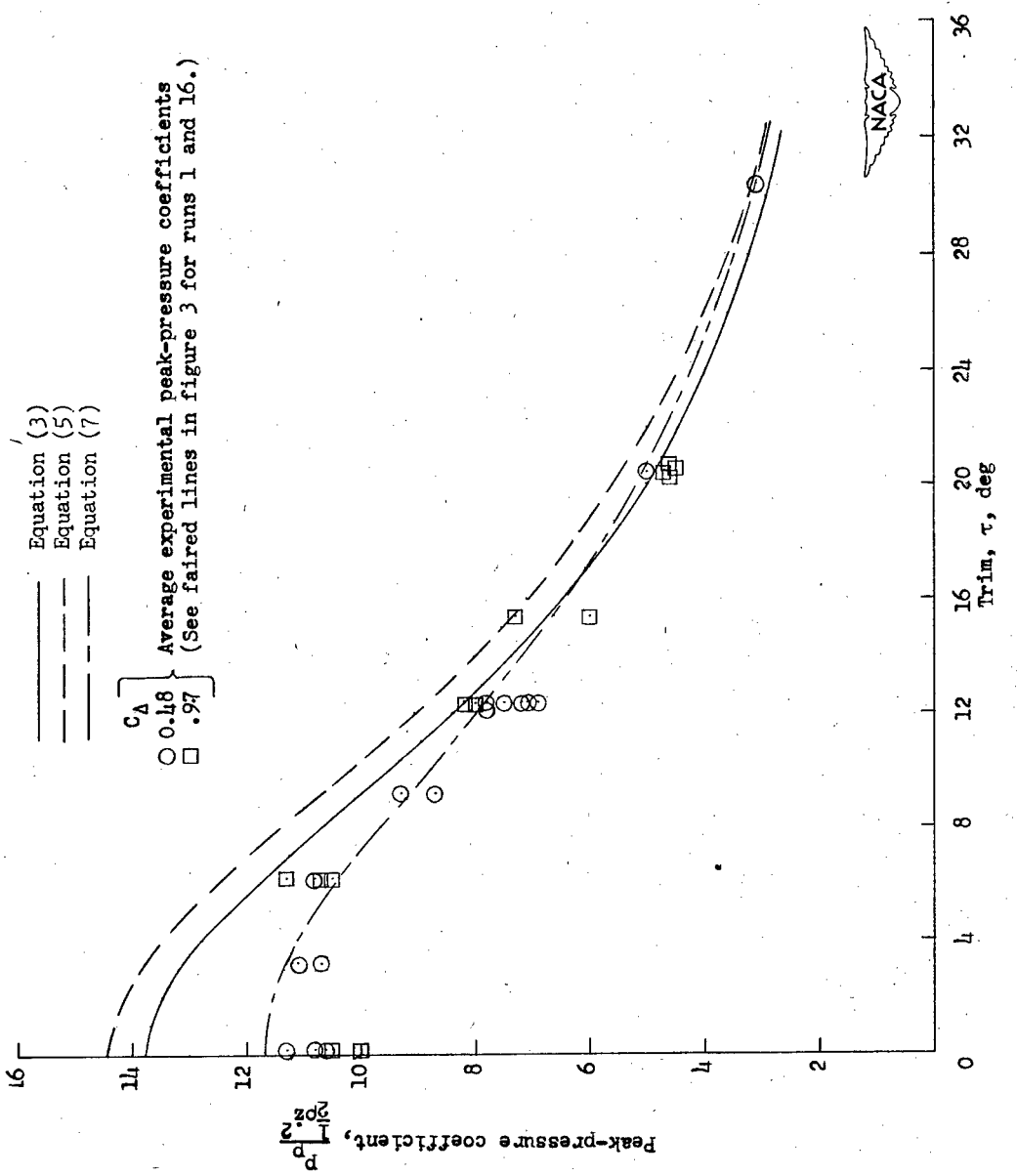
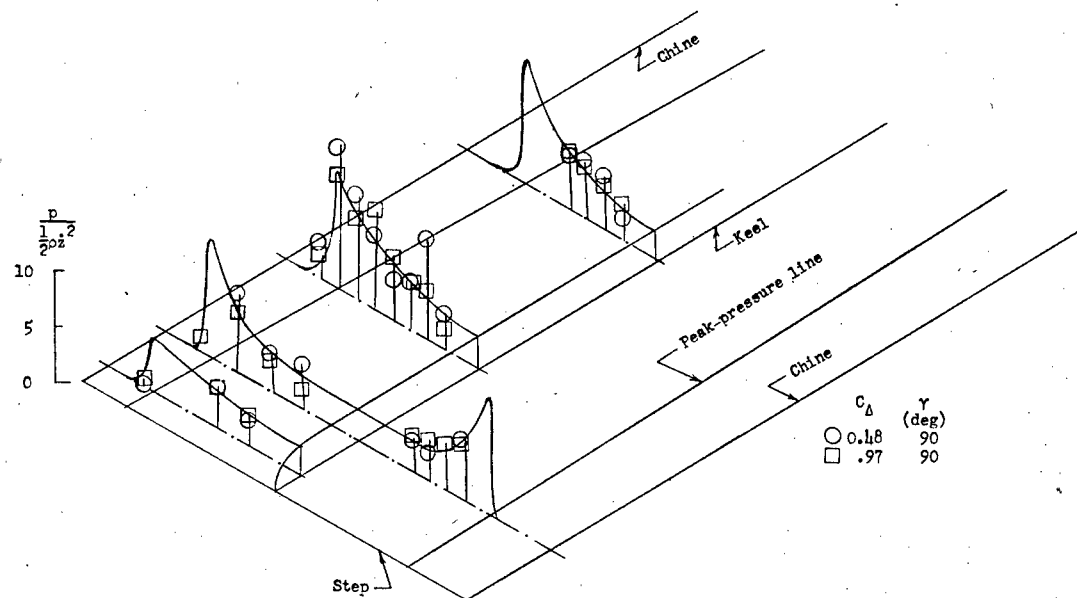
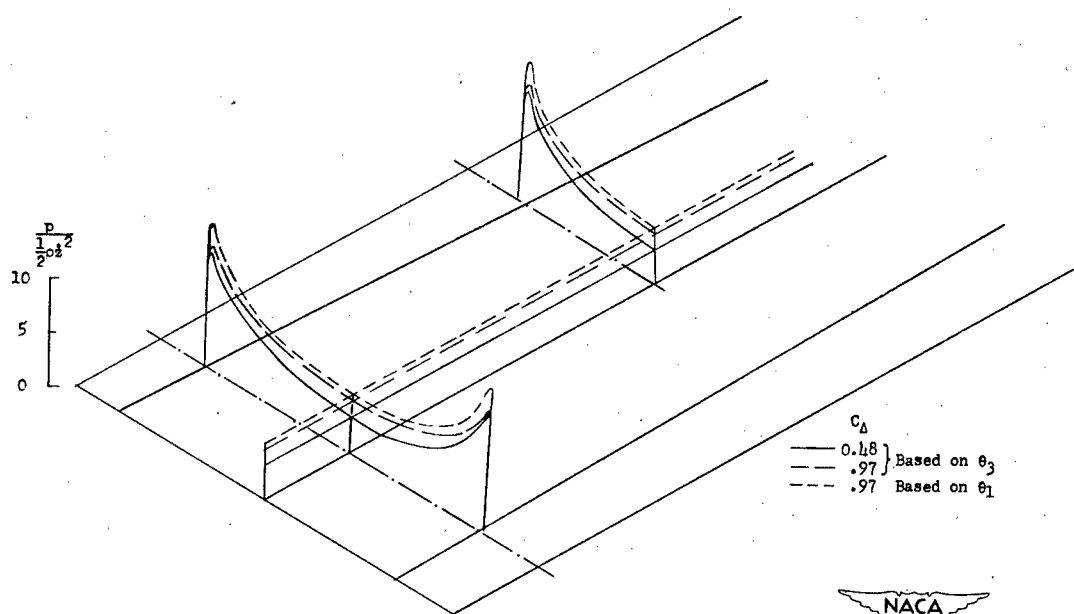


Figure 4.- Experimental and calculated variations of the peak-pressure coefficient with trim.  $\beta = 22\frac{1}{2}^{\circ}$ .



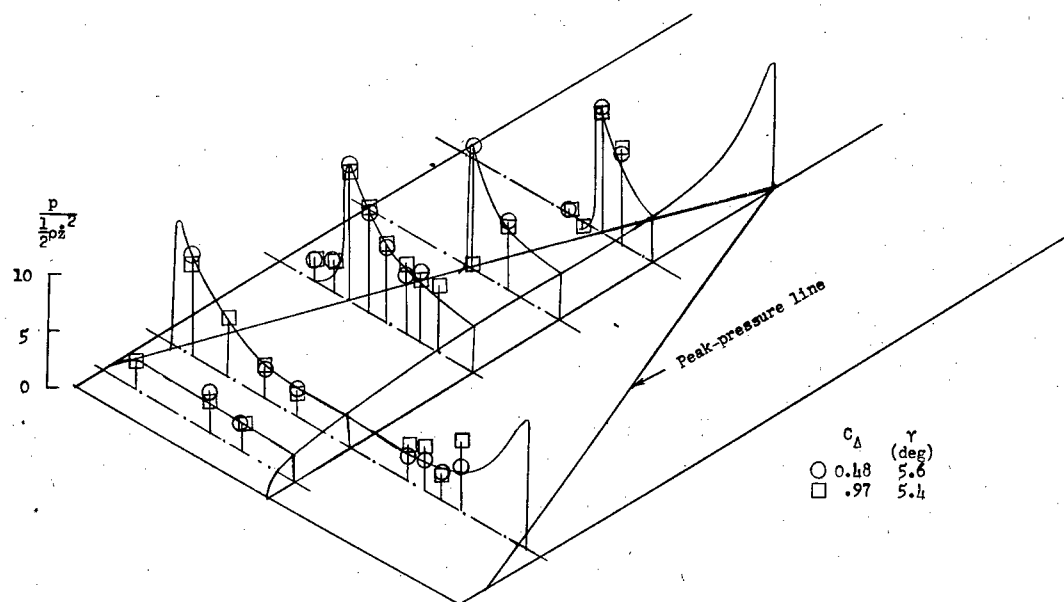
Experimental pressure distributions



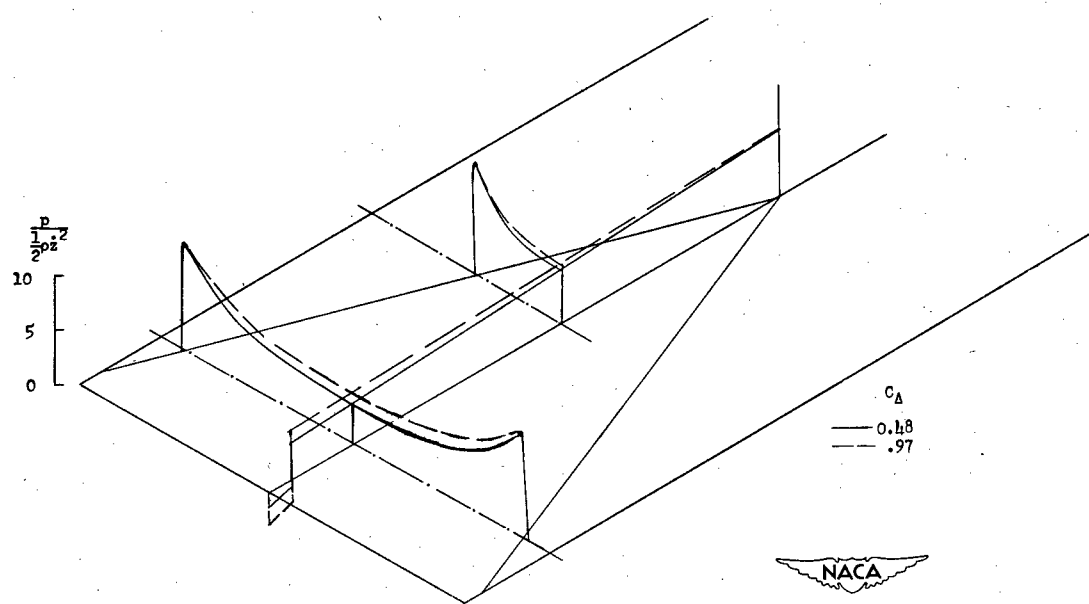
Calculated pressure distributions

(a)  $\tau = 0.2^\circ$ ;  $A \approx 3.$ 

Figure 5.- Experimental and calculated pressure distributions.

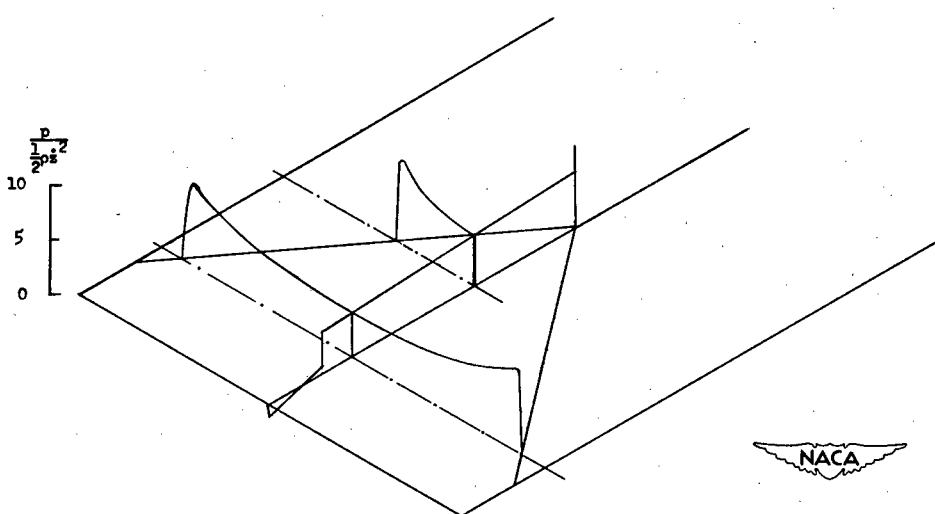
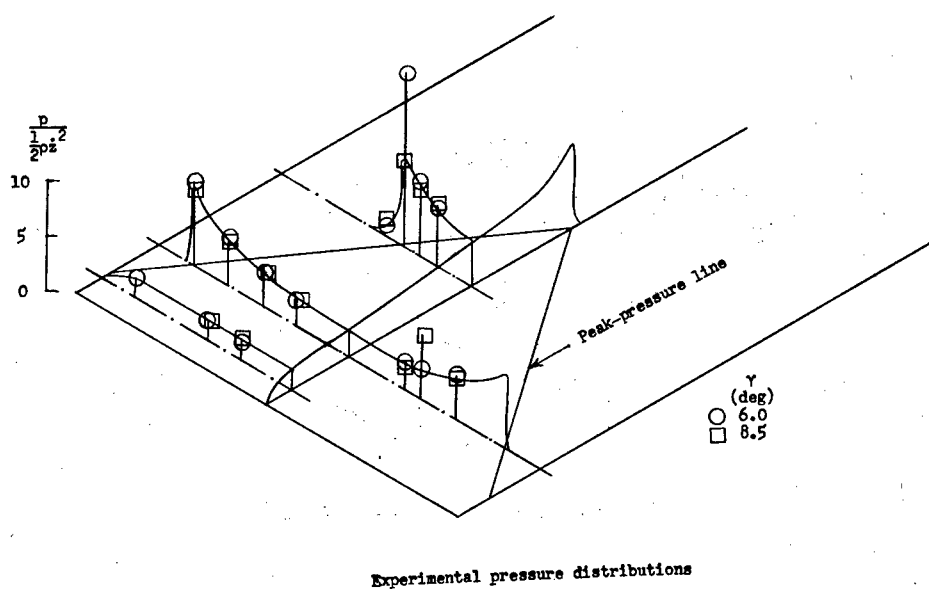


Experimental pressure distributions

Calculated pressure distribution (based on  $\theta_3$ )

$$(b) \quad \tau = 6.3^\circ; \quad A \approx 2.5.$$

Figure 5.- Continued.

Calculated pressure distribution (based on  $\theta_3$ )

$$(c) \quad \tau = 12.4^\circ; \quad C_\Delta = 0.48; \quad A \approx 1.4.$$

Figure 5.- Continued.

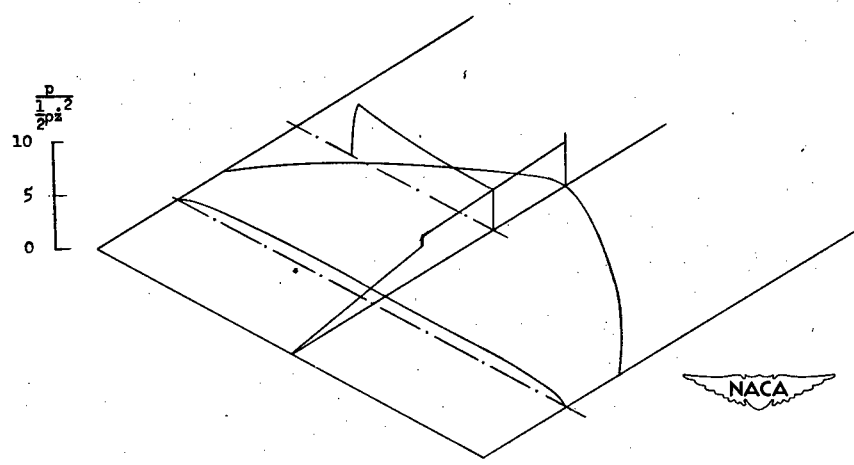
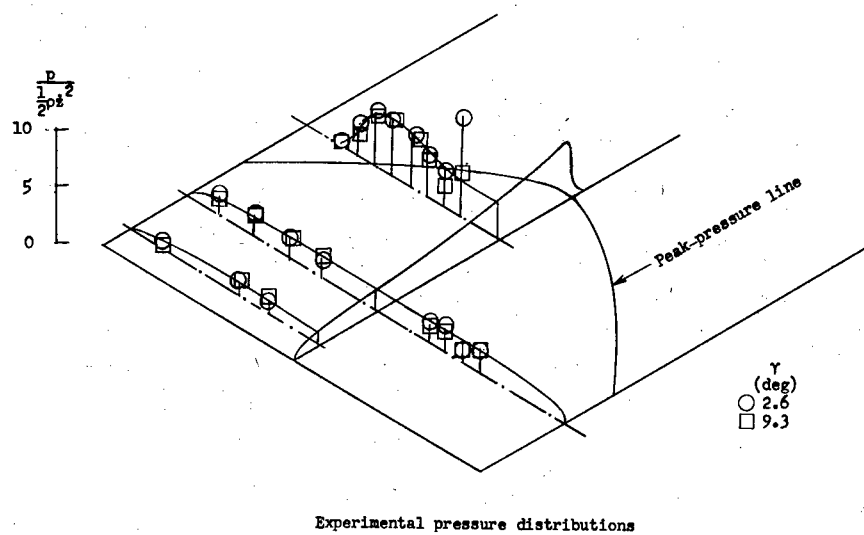
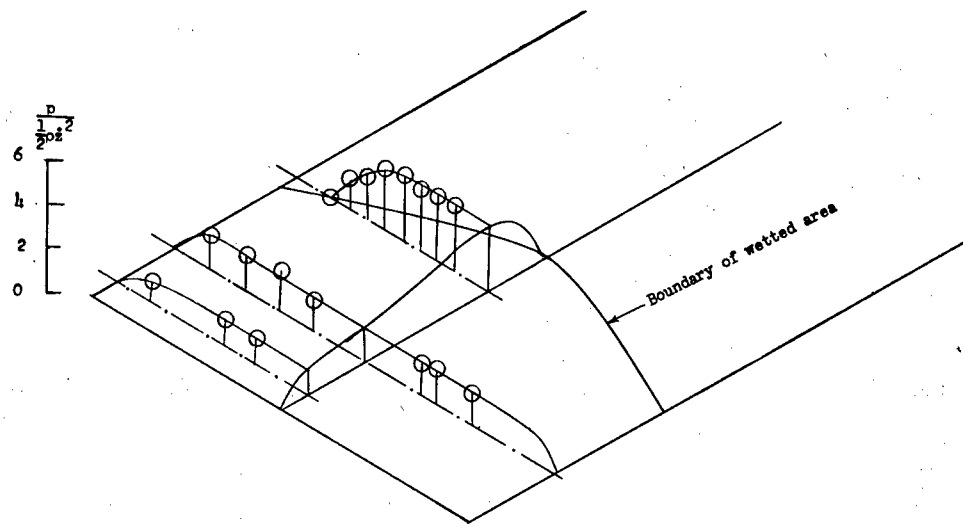
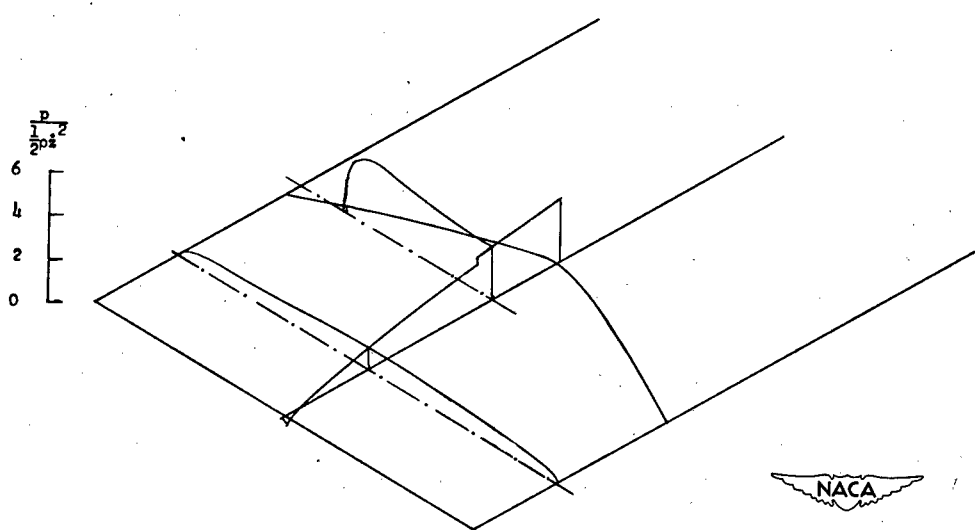
Calculated pressure distribution (based on  $\theta_3$ )(d)  $\tau = 20.5^\circ$ ;  $C_D = 0.97$ ;  $A \approx 0.9$ .

Figure 5.- Continued.



Experimental pressure distributions

Calculated pressure distribution (based on  $\theta_3$ )

$$(e) \quad \tau = 30.3^\circ; C_D = 0.48; A \approx 0.8.$$

Figure 5.- Concluded.

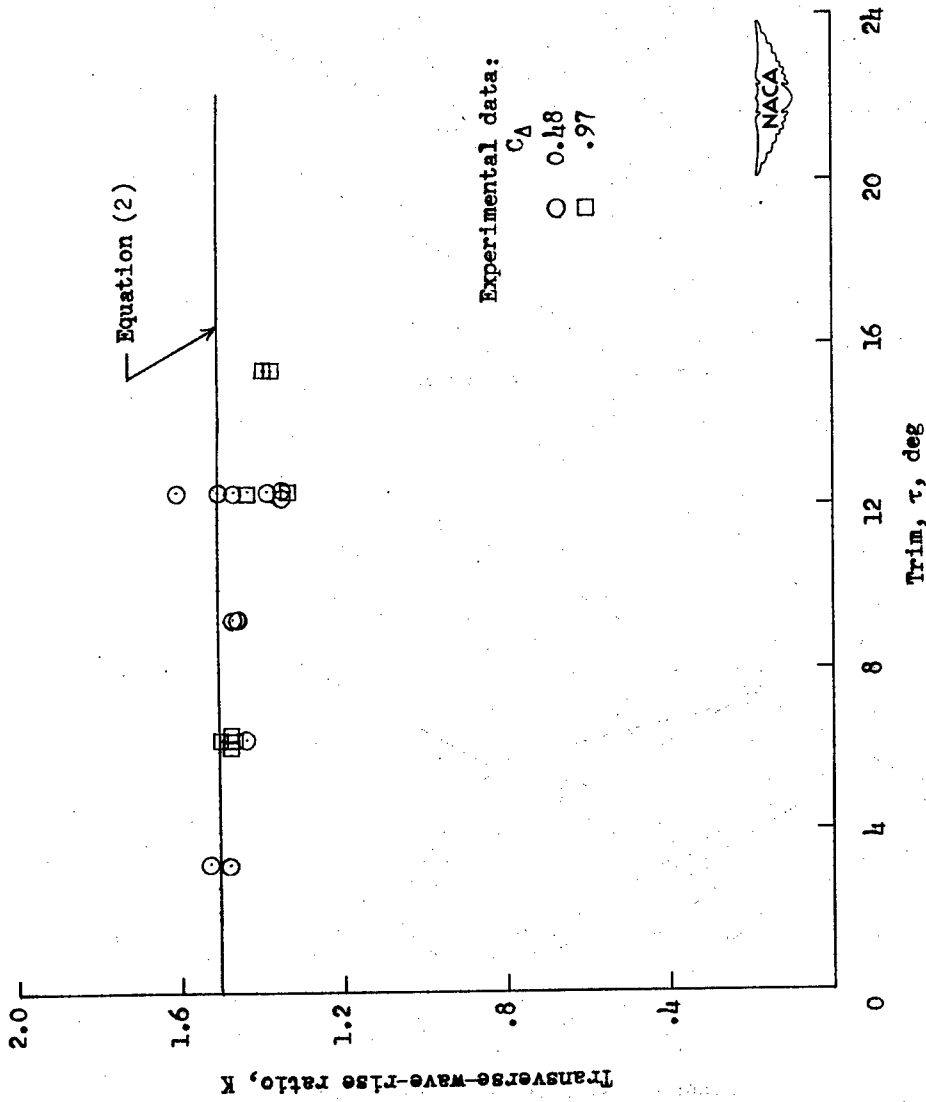
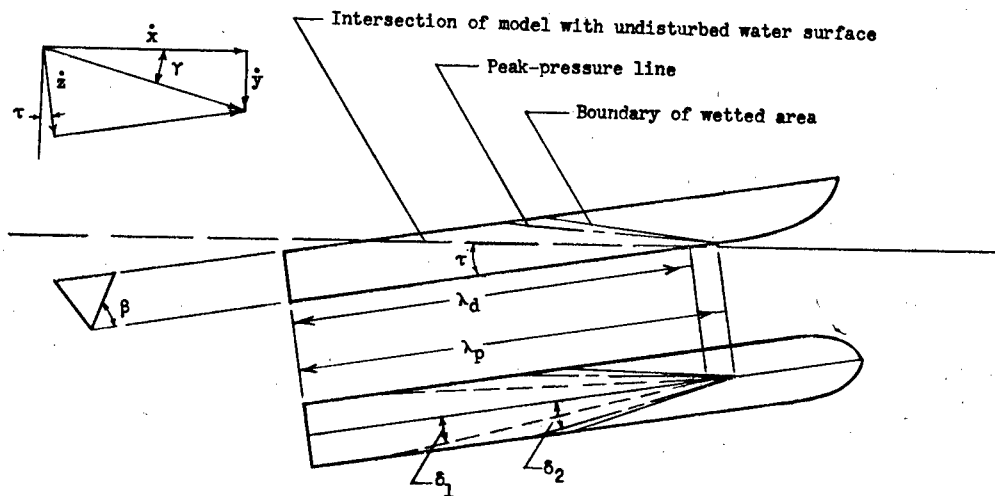
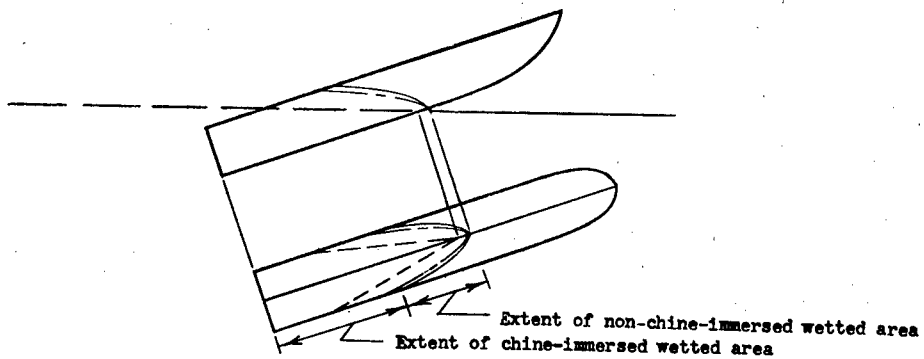


Figure 6.- The transverse-wave-rise ratio  $\left( K = \frac{\tan \delta_2}{\tan \delta_1} \right)$  for a float having

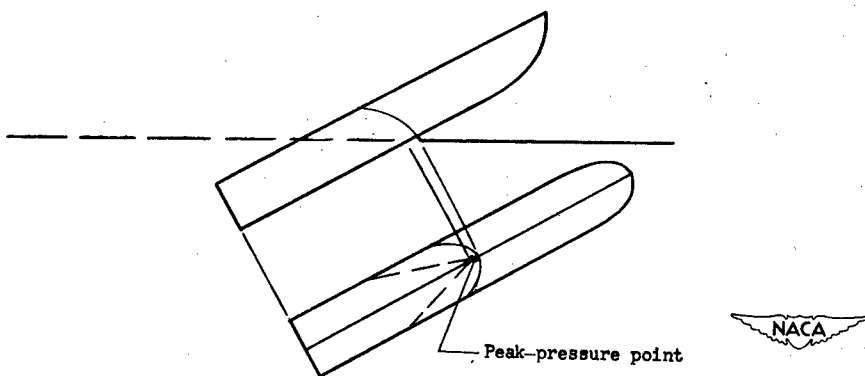
a  $22\frac{1}{2}^0$  angle of dead rise.



(a) Geometry for small trims.



(b) Geometry for large trims.



(c) Geometry for very large trims.

Figure 7.- Wave rise and velocity relations for a prismatic V-bottom surface.

<p><b>NACA TN 2816</b> National Advisory Committee for Aeronautics. WATER-PRESSURE DISTRIBUTIONS DURING LANDINGS OF A PRISMATIC MODEL HAVING AN ANGLE OF DEAD RISE OF 22-1/2° AND BEAM- LOADING COEFFICIENTS OF 0.48 AND 0.97. Robert F. Smiley. November 1952. 37p. diagrs., 6 tabs. (NACA TN 2816)</p> <p>As part of an over-all program, smooth-water landing tests of a prismatic float having an angle of dead rise of 22-1/2° were made. Water-pressure, velocity, draft, and acceleration data are presented. Landings were made for beam-loading coefficients of 0.48 and 0.97 at fixed trims between 0.2° and 30.3° for a range of flight-path angles from 4.6° to 25.9° and also for 90°. The experimental pressure distributions are found to be in fair agreement with the predictions of the available theory; however,</p>	<p>NACA TN 2816 National Advisory Committee for Aeronautics. WATER-PRESSURE DISTRIBUTIONS DURING LANDINGS OF A PRISMATIC MODEL HAVING AN ANGLE OF DEAD RISE OF 22-1/2° AND BEAM- LOADING COEFFICIENTS OF 0.48 AND 0.97. Robert F. Smiley. November 1952. 37p. diagrs., 6 tabs. (NACA TN 2816)</p> <p>As part of an over-all program, smooth-water landing tests of a prismatic float having an angle of dead rise of 22-1/2° were made. Water-pressure, velocity, draft, and acceleration data are presented. Landings were made for beam-loading coefficients of 0.48 and 0.97 at fixed trims between 0.2° and 30.3° for a range of flight-path angles from 4.6° to 25.9° and also for 90°. The experimental pressure distributions are found to be in fair agreement with the predictions of the available theory; however,</p>
<p>Copies obtainable from NACA, Washington (over)</p> <p><b>NACA TN 2816</b> National Advisory Committee for Aeronautics. WATER-PRESSURE DISTRIBUTIONS DURING LANDINGS OF A PRISMATIC MODEL HAVING AN ANGLE OF DEAD RISE OF 22-1/2° AND BEAM- LOADING COEFFICIENTS OF 0.48 AND 0.97. Robert F. Smiley. November 1952. 37p. diagrs., 6 tabs. (NACA TN 2816)</p> <p>As part of an over-all program, smooth-water landing tests of a prismatic float having an angle of dead rise of 22-1/2° were made. Water-pressure, velocity, draft, and acceleration data are presented. Landings were made for beam-loading coefficients of 0.48 and 0.97 at fixed trims between 0.2° and 30.3° for a range of flight-path angles from 4.6° to 25.9° and also for 90°. The experimental pressure distributions are found to be in fair agreement with the predictions of the available theory; however,</p>	<p>Copies obtainable from NACA, Washington (over)</p> <p><b>NACA TN 2816</b> National Advisory Committee for Aeronautics. WATER-PRESSURE DISTRIBUTIONS DURING LANDINGS OF A PRISMATIC MODEL HAVING AN ANGLE OF DEAD RISE OF 22-1/2° AND BEAM- LOADING COEFFICIENTS OF 0.48 AND 0.97. Robert F. Smiley. November 1952. 37p. diagrs., 6 tabs. (NACA TN 2816)</p> <p>As part of an over-all program, smooth-water landing tests of a prismatic float having an angle of dead rise of 22-1/2° were made. Water-pressure, velocity, draft, and acceleration data are presented. Landings were made for beam-loading coefficients of 0.48 and 0.97 at fixed trims between 0.2° and 30.3° for a range of flight-path angles from 4.6° to 25.9° and also for 90°. The experimental pressure distributions are found to be in fair agreement with the predictions of the available theory; however,</p>

NACA TN 2816

NACA TN 2816

better agreement is obtained by modification of the theory.

better agreement is obtained by modification of the theory.

Copies obtainable from NACA, Washington



NACA TN 2816

better agreement is obtained by modification of the theory.

Copies obtainable from NACA, Washington



NACA TN 2816

better agreement is obtained by modification of the theory.

Copies obtainable from NACA, Washington



Copies obtainable from NACA, Washington

